CORA Cork Open Research Archive
Cartlann Taighde Oscailte Chorcaí

Title	Cobalt-based electrode materials for sodium-ion batteries
Authors	Qi, Shihan;Wu, Daxiong;Dong, Yan;Liao, Jiaqin;Foster, Christopher W.;O'Dwyer, Colm;Feng, Yuezhan;Liu, Chuntai;Ma, Jianmin
Publication date	2019-03-19
Original Citation	Qi, S., Wu, D., Dong, Y., Liao, J., Foster, C. W., O'Dwyer, C., Feng, Y., Liu, C. and Ma, J (2019) 'Cobalt-based electrode materials for sodium-ion batteries', Chemical Engineering Journal, 370, pp. 185-207. doi:10.1016/j.cej.2019.03.166
Type of publication	Article (peer-reviewed)
Link to publisher's version	https://www.sciencedirect.com/science/article/pii/S138589471930631X - 10.1016/j.cej.2019.03.166
Rights	© 2019, Elsevier B.V. All rights reserved. This manuscript version is made available under the CC BY-NC-ND 4.0 license. - https://creativecommons.org/licenses/by-nc-nd/4.0/
Download date	2026-11-04 18:09:50
Item downloaded from	https://hdl.handle.net/10468/7688



UCC
University College Cork, Ireland
Coláiste na hOllscoile Corcaigh

Accepted Manuscript



Review

Cobalt-Based Electrode Materials for Sodium-Ion Batteries

Shihan Qi, Daxiong Wu, Yan Dong, Jiaqin Liao, Christopher W. Foster, Colm O'Dwyer, Yuezhan Feng, Chuntai Liu, Jianmin Ma

PII: S1385-8947(19)30631-X
DOI: https://doi.org/10.1016/j.cej.2019.03.166
Reference: CEJ 21290

To appear in: *Chemical Engineering Journal*

Received Date: 16 January 2019
Revised Date: 25 February 2019
Accepted Date: 18 March 2019

Please cite this article as: S. Qi, D. Wu, Y. Dong, J. Liao, C.W. Foster, C. O'Dwyer, Y. Feng, C. Liu, J. Ma, Cobalt-Based Electrode Materials for Sodium-Ion Batteries, *Chemical Engineering Journal* (2019), doi: https://doi.org/10.1016/j.cej.2019.03.166

This is a PDF file of an unedited manuscript that has been accepted for publication. As a service to our customers we are providing this early version of the manuscript. The manuscript will undergo copyediting, typesetting, and review of the resulting proof before it is published in its final form. Please note that during the production process errors may be discovered which could affect the content, and all legal disclaimers that apply to the journal pertain.

ACCEPTED MANUSCRIPT

Cobalt-Based Electrode Materials for Sodium-Ion Batteries

Shihan Qi,[a] Daxiong Wu,[a] Yan Dong,[a] Jiaqin Liao,[a] Christopher W. Foster,[b,*] Colm O'Dwyer,[c,d,e*] Yuezhan Feng,[f] Chuntai Liu[f] and Jianmin Ma[a, f,*]

[a]*School of Physics and Electronics, Hunan University, Changsha 410082, P.R. China*

[b]*Faculty of Science and Engineering, Manchester Metropolitan University, Manchester, Chester Street, M15 GD, UK*

[c] *School of Chemistry, University College Cork, Cork, T12 YN60, Ireland*

[d] *Tyndall National Institute, Lee Maltings, Cork, T12 R5CP, Ireland*

[e] *Environmental Research Institute, University College Cork, Lee Road, Cork T23 XE10, Ireland*

[f]*Key Laboratory of Materials Processing and Mold (Zhengzhou University), Ministry of Education, Zhengzhou University, Zhengzhou, 450002, China*

Corresponding authors: Christopher W. Foster, Colm O'Dwyer or Jianmin Ma

Email addresses:

cwfoster90@gmail.com (Dr. Foster)

c.odwyer@ucc.ie (Prof. O'Dwyer)

nanoelechem@hnu.edu.cn (Prof. Ma)

ACCEPTED MANUSCRIPT

ACCEPTED MANUSCRIPT

Abstract

The demand for grid-scale energy storage systems has rapidly grown over recent years, to meet the requirements of structural innovation within the energy industry. Due to their inexpensive manufacturing and operating costs, and the similar electrochemical mechanism with the well-established lithium-ion batteries (LIBs), sodium ion batteries (SIBs) have been considered as an attractive candidate for grid-scale energy storage systems. A variety of cobalt-based cathode and anode materials, including cobalt oxides, cobalt chalcogenide and layered sodium cobaltate, have been synthesized and evaluated for sodium storage within the academic literature. In this article, we present a comprehensive review of the recent progress with cobalt-based electrodes (both as an anode and cathode material) used in SIBs. In detail, the electrochemical mechanisms, advantages and disadvantages, the relationship between crystalline structure and electrochemical performance and strategies to enhance the overall electrochemical performance of cobalt-based cathode and anode materials are discussed. Up to now, some cathode materials have already reached a high energy density, which is comparable to commercial LIBs. Furthermore, some cobalt-based materials can maintain a high Coulombic efficiency of over 99% with high reversible capacity during long cycling life. These encouraging results, allow such cobalt-based electrode materials to be a potential solution for grid-scale SIB systems.

Keywords: Sodium-ion batteries; Anode; Cathode; Cobalt oxides; Cobalt chalcognides

ACCEPTED MANUSCRIPT

ACCEPTED MANUSCRIPT

1. Introduction

With the current alarming global pollution problem, the need to develop green renewable energies, and to reduce pollutant emission, is becoming more demanding and is one of the most pressing issues of this generation. As alternatives to traditional fossil energies, solar power, wind power, tidal power and other green energy technologies have rapidly developed over the last decade. As a result, this trend has led to a demand for new energy storage technologies, especially within stationary applications.[1-5] Among the current energy storage technologies, the lithium-ion battery (LIB) has achieved great success, in particular within portable electronic equipment, and is predicted to dominate the electric vehicle market.[6-10] However, the limited reserves and ever-increasing cost of lithium and other critical raw materials casts doubt over whether this technology is also suitable for large-scale stationary applications. With abundant resource of sodium in both the earth's crust and oceans, the cost of sodium-containing materials is significantly lower than its lithium competitor.[11-14] For example, one of the most common sodium resource, Trona (Na_2CO_3), is ~20-30 times cheaper than Li_2CO_3.[15] However, it should be noted that the weight of Na is three times higher than Li. Besides, the standard electrochemical potential of Na is lower than Li (2.71 V for Na and 3.04 V for Li, *vs*. SHE).[16] These intrinsic properties result in a lower energy density for the sodium-ion battery (SIBs) over that of the LIB under similar conditions. Thus, SIBs have been regarded as a promising candidate for stationary energy storage devices, which is evident in the research of this technology over the last decade.[17-20]

Unfortunately, however, the Na^+ ion does have a larger radius (1.06 Å) than that of the Li^+ ions (0.76 Å), which in general will cause some problems for SIB materials.[16] The larger radius creates unstable cathodes and anodes during charge/discharge process, leading to a hindered cycling performance.[17, 18] Additionally, the Na^+ ion possesses a larger energy barrier for insertion into many electrode materials, which could conceivably pose a problem of limited capacity and poor rate capability. For example, graphite with a layer spacing of 3.35 Å, only shows a low irreversible capacity for SIBs. Until now, these inferior cycling performances and rate capabilities still hinder the practical application of SIBs.[21, 22] To develop suitable electrode materials with an enhanced electrochemical performance is one of the key issues for the further advancement of SIBs.[23-27] An amount of materials have been studied as electrode materials for

ACCEPTED MANUSCRIPT

SIBs with a few offering acceptable electrochemical performance. For cathode materials, most research focuses upon layered metallic oxides (Na_xMO_2, M=Mn,[15] Co,[28, 29] Ni,[30] Fe,[31] Cr,[32] etc), phosphates ($NaFePO_4$,[33] $Na_3V_2(PO_4)_3$,[34] $NaVPO_4F$,[14] $Na_3V_2(PO_4)_2F_3$,[35] $Na_{1.5}VOPO_4F_{0.5}$,[36] Na_2FePO_4F,[37] etc), transition metal fluorides ($NaMF_3$, M = Fe,[38] Mn, V and Ni[39]), and organic cathodes[40]. For anode materials, hard carbon,[24] metal alloys,[41] metal oxides[42] and chalcogenides[43, 44] are promising candidates.

Cobalt, the 27th element assigned to group VIII B, is a popular metal within material science. Cobalt-based materials have attracted much attention within many fields, including catalysis,[45] thermopower,[46] ferromagnetic properties,[47] energy storage[48-52] to name a few. Especially, for LIBs, $LiCoO_2$ is one of the most successful commercialized cathode materials.[53] Similarly, cobalt-based materials can also play an important role in cathode and anode materials for SIBs.[54-59] The SIB cathode material, Na_xCoO_2 is being investigated primarily because of the commercial success of $LiCoO_2$ in the LIB.[60, 61] With respect to anode materials, cobalt oxides[62-64] and cobalt chalcogenides[65-68] demonstrate a high theoretical capacity for sodium storage. Full cell pairings of stable materials remain to be found and commercialized for SIBs.

We report a detailed review of the most recent advancements in cobalt-based materials for SIBs, with a focus on both cathode and anode electrode materials. This review covers the electrochemical mechanisms, a comparison of advantages and disadvantages, the relationship between crystalline structure and electrochemical performance, and strategies to enhance the overall electrochemical performance of cobalt-based cathode and anode materials. Finally, an overall outlook containing key challenges and perspectives on the future development of SIBs is provided.

2. Cobalt Oxide Anodes

2.1 Co_3O_4

Over the last decade, transition metal oxides (TMOs) have been core materials central to developments in semiconductor technologies, catalysis, sensing and energy storage to name a few. In particular, many TMOs, including Fe_2O_3,[69] Co_3O_4,[70] MoO_3,[71] TiO_2,[72] etc, are regarded as promising candidates for the replacement of graphite anodes in batteries, due to their high alkaline ion storage capacity, for example Co_3O_4 possesses a high theory capacity of 890 mAh

ACCEPTED MANUSCRIPT

g^{-1}.[73] However, Co_3O_4 does possess an array of limitations, which is currently hindering its application as an anode material, such as limited electrical conductivity, poor ion diffusion kinetics, large volume expansion during Na^+ ion insertion and so on.[74, 75] Nanocrystallization and protective coating layer are generally considered as an effective methodology to enhance the electrochemical performance of Co_3O_4. Based on such viewpoint, a large number of nano-sized Co_3O_4 and Co_3O_4/C composites with various morphologies such as nanospheres,[76, 77] nanotubes,[78] hollow octahedra,[79] etc. have been reported within the literature.

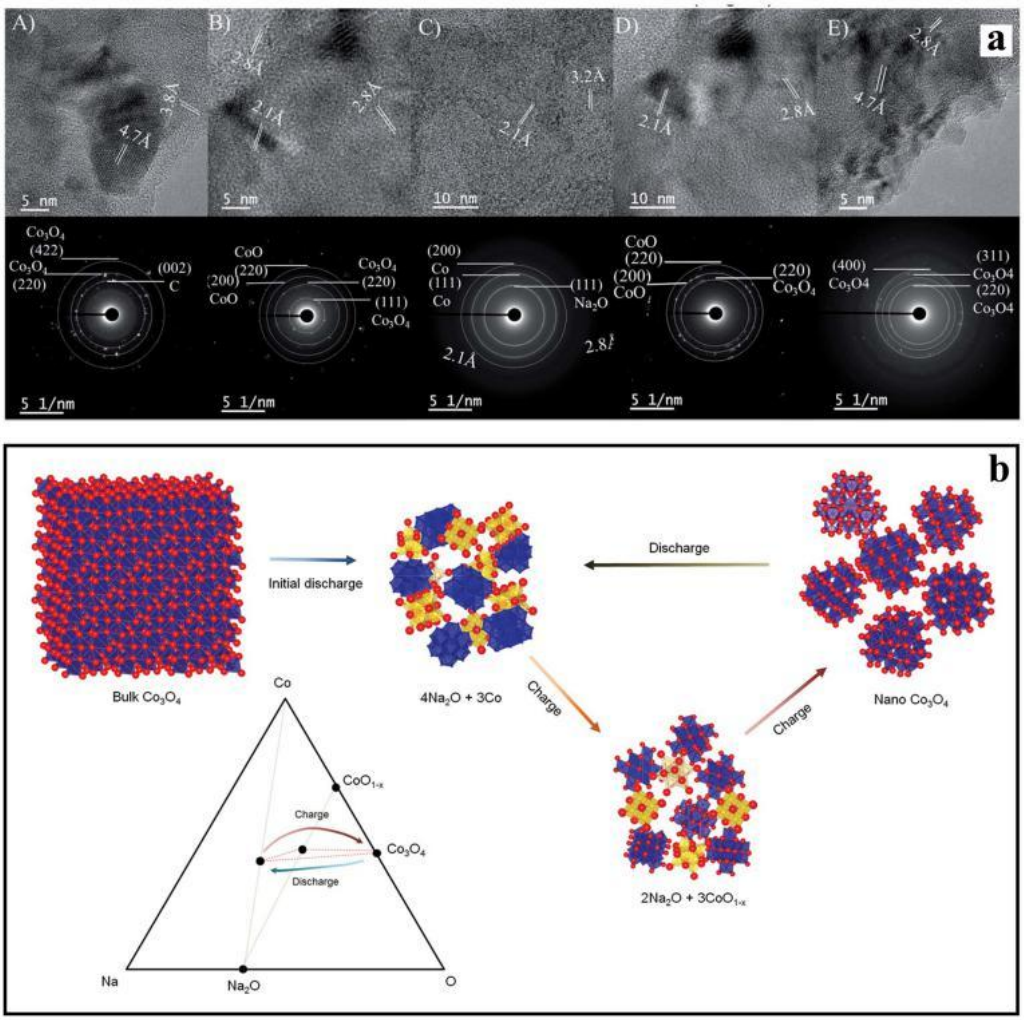


Fig. 1 Structural evolution of the Co_3O_4@NC electrode during the electrochemical reaction. (a) TEM images (top) and selected area electron diffraction (SAED) patterns (bottom) at the corresponding points: A) pristine state, B) the discharged state at 0.6 V, C) fully discharged state at 0.01 V, D) the charged state at 1.4 V and E) the fully charged state at 3.0 V.[80] (b) Schematics of conversion and reconversion reaction mechanism for Co_3O_4 in Na rechargeable batteries.[81]

ACCEPTED MANUSCRIPT

As an anode material for sodium ion battery, Co_3O_4 goes through a conversion reaction during charge/discharge process.[80, 81] As can be seen in Fig 1a, the structural evolution of this material has been investigated systematically by ex-situ TEM and selected area electron diffraction (SAED) at different charge/discharge states. In detail, upon the Na^+ ion insertion, the Co_3O_4 phase gradually turns into a new phase of CoO over the voltage range of 3.0-0.6 V. In the fully discharged state at 0.01 V, only Co and Na_2O can be detected. Upon the subsequent charge process, the phases of CoO and Co_3O_4 emerge at 1.4 V and only the Co_3O_4 phase exists after fully charging at 3.0 V. Based upon these results, the conversion reaction during discharge process of Co_3O_4 with Na^+ ion can be summarized as:

$$Co_3O_4 + 2Na^+ + 2e^- \rightarrow 3CoO + Na_2O$$

$$3CoO + 6Na^+ + 6e^- \rightarrow 3Co + 3Na_2O$$

It is well reported that bulk Co_3O_4 material, upon the charge/discharge, undergoes a morphological deterioration as the particle size reduces on the conversion reaction, (as demonstrated in Fig 1b)[81]. This effect lowers the electronic conductivity of the electrode, and can even result in the loss of active material. Such increases in surface area (due to the decreasing particle size) prevent the formation of a stable SEI membrane, often requiring SEI reformation to some degree in every cycle. To understand the morphological-performances correlations of Co_3O_4 materials, micro-sized Co_3O_4 slabs, nano-sized Co_3O_4 needles and nano-sized Co_3O_4 flakes were synthesized by Ruffo's group.[82] It is obvious from their data that the Co_3O_4 needles have the highest capacity and best cycling performance among them. It is believed that smaller size and larger surface area provides a shorter ion diffusion pathway and an increased availability of Na^+ adsorption active sites, which leads to a higher capacity. In this case, the increase in grain boundary resistance with size reduction was not reported as a limiting factor in performance. Presumably, the nanoparticles are capable of withstanding the electrode stress caused by the material expansion.[83]

Another example within the literature to improve the stability of these metal oxides is their growth on conductive carbon substrates.[84-86] Recently, a form of Co_3O_4 mesoporous nanosheets/3D graphene composite (Co_3O_4 MNSs/3DGN), with an average pore size of about 40 nm, was reported.[87] As displayed in Fig 2a-b, the introduction of graphene improves the overall

ACCEPTED MANUSCRIPT

conductivity of the composite and buffers the volume change of the cobalt oxide with the porous nanosheet structure benefiting the diffusion of Na^+ ions. As a result, this composite demonstrates an improved cycling performance and rate capability compared to Co_3O_4 nanosheets and Co_3O_4 nanoparticles. Using a Co-based MOF as a precursor to synthesize Co_3O_4/carbon composites is another effective method. For example, several Co_3O_4 with a N-doped carbon coating composites have been reported within the literature.[88]

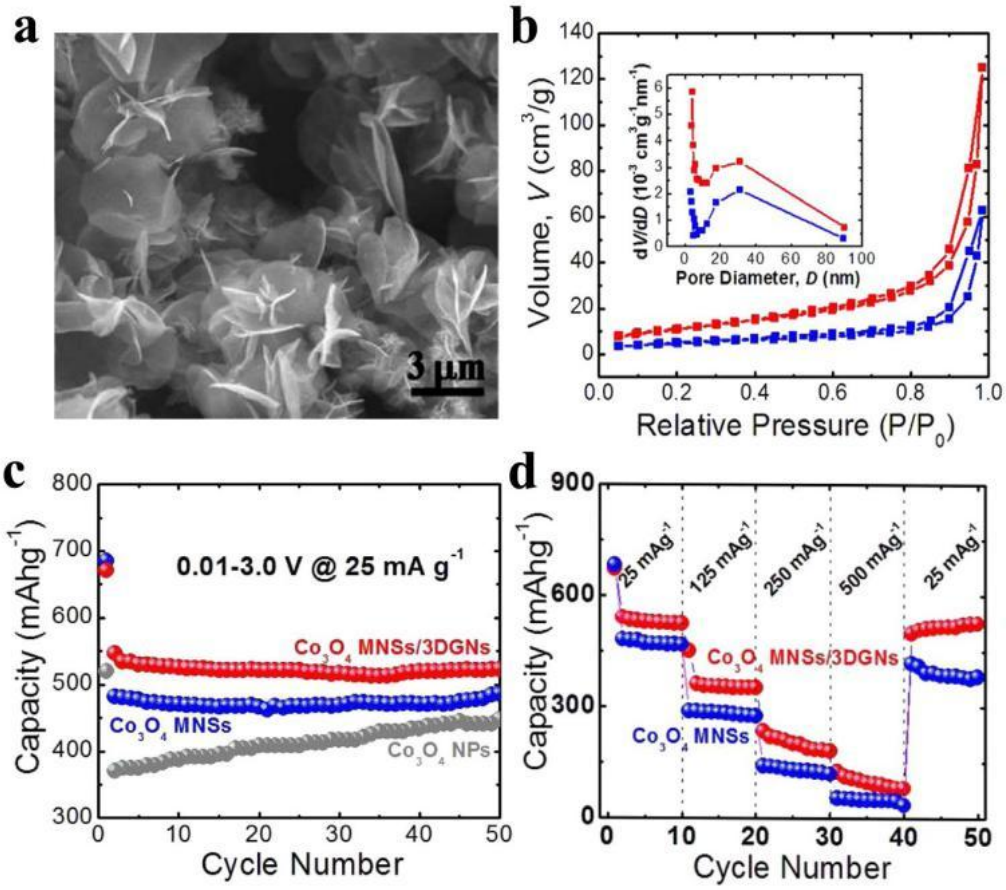


Fig. 2 Structural characterizations and electrochemical performances of Co_3O_4 MNSs/3DGN. (a) FESEM image and (b) Nitrogen adsorption/desorption isotherms for Co_3O_4 MNSs/3DGNs nanohybrids (red lines) and Co_3O_4 MNSs (blue lines). Inset: corresponding pore size distribution curves. (c) The cycling performance of Co_3O_4- MNSs/3DGNs nanohybrids and Co_3O_4 MNSs. (d) Rate capability of the Co_3O_4-MNSs/3DGNs nanohybrids and Co_3O_4 MNSs electrodes.[87]

Recently, some papers have proven that Co_3O_4/metal oxide heterostructures also show good electrochemical performance in sodium ion batteries.[89] is the rationale considered that an oxide

ACCEPTED MANUSCRIPT

heterostructure could potentially improve interfacial and surface charge transfer during charging and discharging. Thus, the composite with a heterostructure should possess a high electrical conductivity. For example, a novel graphene/SnO_2/Co_3O_4 (GSC) heterojunction material has been reported.[90] In detail, the Co_3O_4 is a p-type semiconductor with a band gap of 2.2 eV and SnO_2 is an n-type semiconductor with a wider band gap of 3.8 eV. In the discharge process, the direction of the internal electric field should point from the SnO_2 side to Co_3O_4 side as an effective p-n junction. Based on the inbuilt depletion region, the accumulation of charge at the interfaces can be reduced. This is beneficial to the Na^+ ion's diffusion and insertion into this material, as shown in Fig. 3a according to the authors. A smaller charge transfer impedance of the graphene/SnO_2/Co_3O_4 composite compared to the graphene/SnO_2 (GS) can be observed. As a result, graphene/SnO_2/Co_3O_4 demonstrates better cyclic performance than the composite without a heterostructure. The same trend can also be obtained with ZnO/Co_3O_4[91] and Co_3O_4/MnO_2[92] composites. In addition, doping with metallic ions (such as Zn^{2+} and Ni^{2+}) is another effective way to enhance the sodium storage properties.[93]

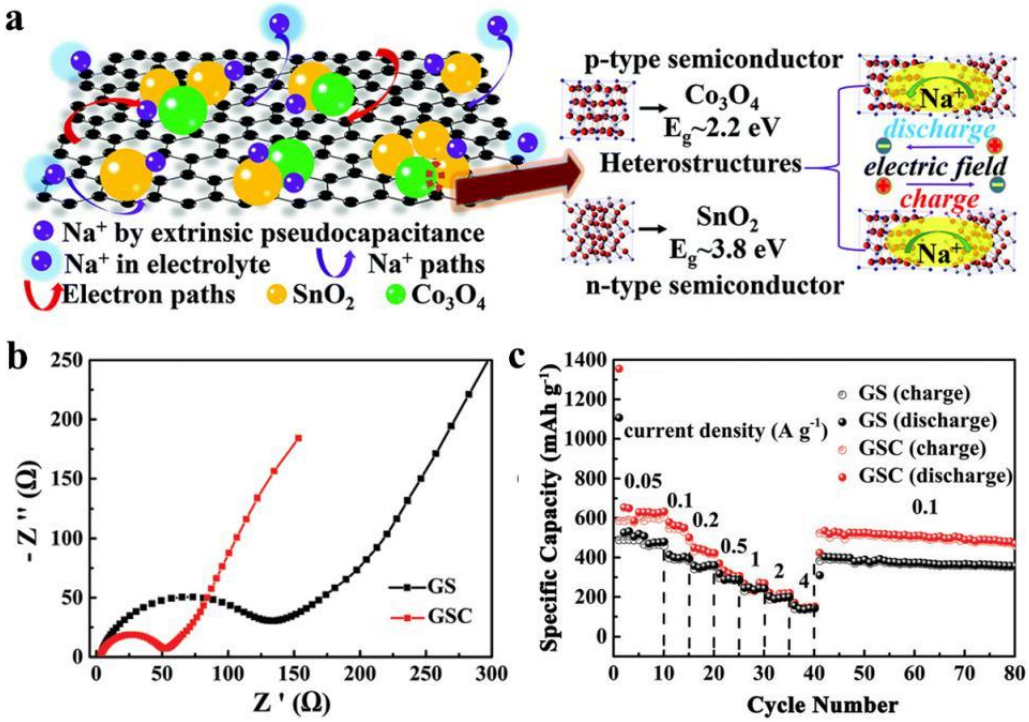


Fig. 3 (a) Summary of the enhanced high-rate capacity mechanism of the GSC anodes in the Na-ion battery system. (b) The Nyquist plots of GSC and GS. (c) Rate performance of GSC and GS at applied various current densities.[90]

ACCEPTED MANUSCRIPT

2.2 CoO

Besides Co_3O_4, several recent reports have focused on CoO for application in a sodium ion battery. During the Na^+ insertion process, the electrochemical reaction of CoO can be concluded as the following[94]:

$$CoO + 2Na^+ + 2e^- \rightarrow Co + Na_2O$$

Based on this above reaction, CoO exhibits a sodium storage capacity of 715 mAh g^{-1}.[95] The short cycling life and terrible rate capability also challenge the development of the CoO electrode for the sodium ion battery. To address these limitations, a porous Ni-doped Co/CoO/carbon composite was recently reported.[96] Due to a stated synergistic effect of the carbon coating, highly porous structure, and defect sites caused by Ni-doping, the structural stability, electric and ionic conductivity are improved simultaneously. This material demonstrates a capacity of 307 mAh g^{-1} at 0.1 A g^{-1} and a relatively high discharge capacity of about 280 mAh g^{-1} is observed after 100 cycles at the same current density.

3. Cobalt Sulfide Anodes

3.1 Co_9S_8

Co_9S_8 has attracted great attention over a range of fields of research including catalysis, sensing and energy storage, due to its unique physical and electrochemical properties.[97] As can be seen in Fig 4, cubic Co_9S_8 has a space group of Fm-3m, and a large unit cell parameter of a = 9.926 Å. As shown in Fig 4, its crystal structure comprises two different polyhedra, CoS_6 octahedra and CoS_4 tetrahedra, respectively.[98] In a perfect crystal structure, every CoS_6 octahedron shares its corners with 24 CoS_4 octahedrons. There are three different Co-S bonds with varying bond lengths and energy. This form of structure can not only provide channels for ionic diffusion, but also offers multiple possible routes of bonding-breaking.

ACCEPTED MANUSCRIPT

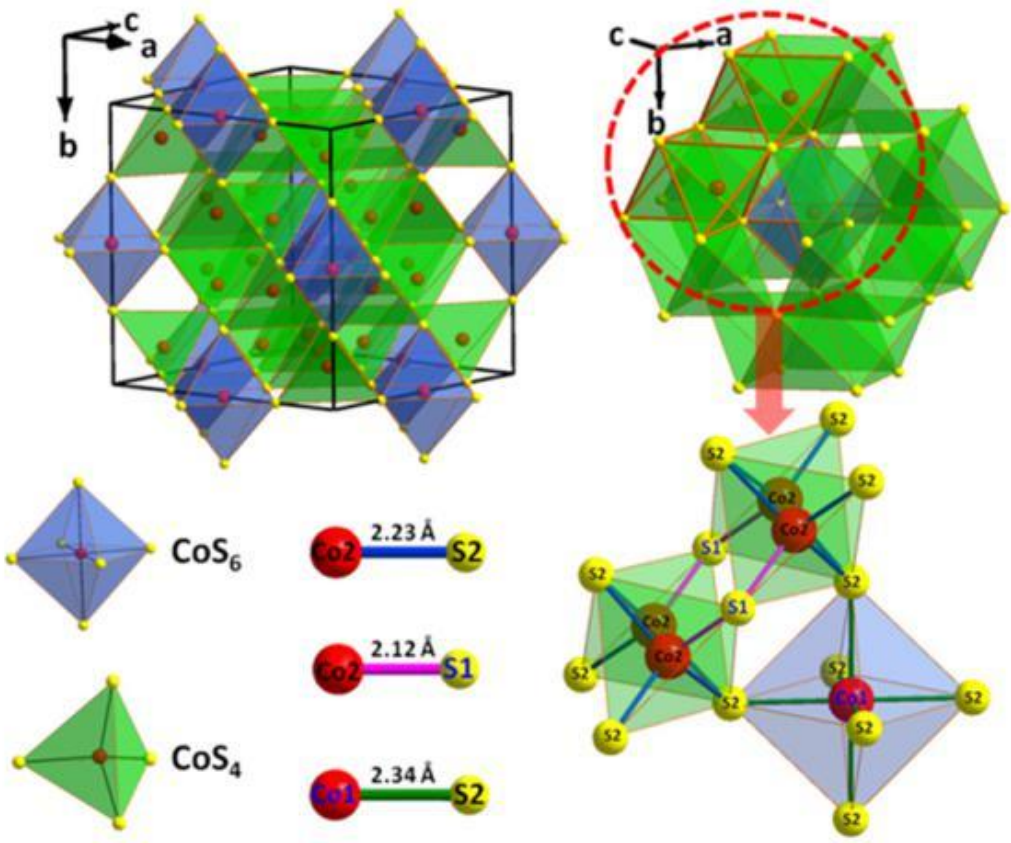


Fig. 4 Schematic structure of cube Co_9S_8.[98]

Through different synthesis methods, such as solvothermal and solid state recrystallization, Co_9S_8-based materials with various morphologies have been obtained.[99, 100] In the energy storage field, engineering these structures to have a large surface area and be capable of high capacity alkaline ion storage properties, nano-sized Co_9S_8 has been widely studied as an electrode material for supercapacitor and lithium ion battery applications. When applied to sodium ion battery systems, Co_9S_8 suffers a conversion reaction according to $Co_9S_8 + 16\ Na^+ \rightarrow 9\ Co + 8\ Na_2S$, which shows a relatively high theoretical capacity of 544 mAh g^{-1}.[101] However, the low degree of reversibility and excessive volume changes caused by the above conversion reaction leads to very poor cycling performance and rate capability, in addition to the unstable solid electrolyte interphase, which also aggravates this problem.[102]

To enhance the electrochemical performance of Co_9S_8 as an anode for sodium ion batteries, several strategies have been reported. For example, hierarchical nanostructuring can play a vital

ACCEPTED MANUSCRIPT

role for a conductive substrate, buffering the stress caused by the change in volume and offer open channels for Na^+ ion diffusion and for mass transport of other reactants in conversion mode processes. Novel Co_9S_8 quantum dots embedded into hierarchical porous carbon frameworks (3DOM Co_9S_8-QDs@NC) was obtained by a template method, as shown in Fig 5a.[99] The SiO_2 nanospheres were utilized as a sacrificial template and were etched to form macropores with an average size of 150 nm and the surface-immobilized Co_9S_8 quantum dots are ~3 nm (Fig 5b) in size. This composite exhibits an improved cycling performance and rate capability compared to the Co_9S_8/C (Co_9S_8-QDs@NC) without hierarchical structure by ensuring good interfacial contact and QD access to the electrolyte. In detail, as can be seen in Fig 5c, when the current density reaches to 10 A g^{-1}, this composite still shows a remarkable specific capacity of 253 mAh g^{-1}. Moreover, a capacity of more than 340 mAh g^{-1} is achieved after 2000 cycles with the Coulombic efficiency of over 99%, at a current density of 1 A g^{-1}. Beyond all the above-mentioned reasons of hierarchical structure, the high ratio of diffusion-controlled capacity is another significant reason for the improved electrochemical performance.

Utilizing a Co-based MOF as the precursor is another effective way to synthesize a hierarchical Co_9S_8-based material. Several studies have proved that ZIF-67 is the suitable precursor for this strategy. For instance, recently, a Co_9S_8 quantum dot/hollow carbon matrix/graphene aerogel was synthesized with the ZIF-67 precursor.[102] This composite demonstrated a stable cycling life over 500 cycles at a current density of 300 mA g^{-1}. Similarly, most capacity is contributed by the diffusion-controlled electrochemical behavior.

Combining with other metal sulfides to form heterostructures can also enhance the sodium storage capacity of Co_9S_8. MoS_2 is another alternative anode material for SIB. For good wettability with organic electrolyte, MoS_2 can play a role as a useful coating layer for other materials.[27] A type of Co_9S_8 core-MoS_2 shell composite (Co_9S_8/MoS_2-CN) shows more stable cycling life and better rate capability than pure Co_9S_8 or pure MoS_2, as shown in Fig 5f-g.[103] It is believed that MoS_2 shell can bring such advantages: smaller Ohmic resistance, lower activation energy for Na^+ ion diffusion and larger exposed surface to the electrolyte, which leads to an improved electrochemical performance. In addition, of the choice of electrolyte will have a significant impact on the sodium storage capacity of a Co_9S_8 electrode. It has been reported that an ether-based electrolyte, such as 1.0 M sodium trifluomethanesulfonate ($NaCF_3SO_3$) dissolved in

ACCEPTED MANUSCRIPT

tetraethylene glycol dimethyl ether (TEGDME), can bring a much more stable long-term cycling life and good rate capability.[100]

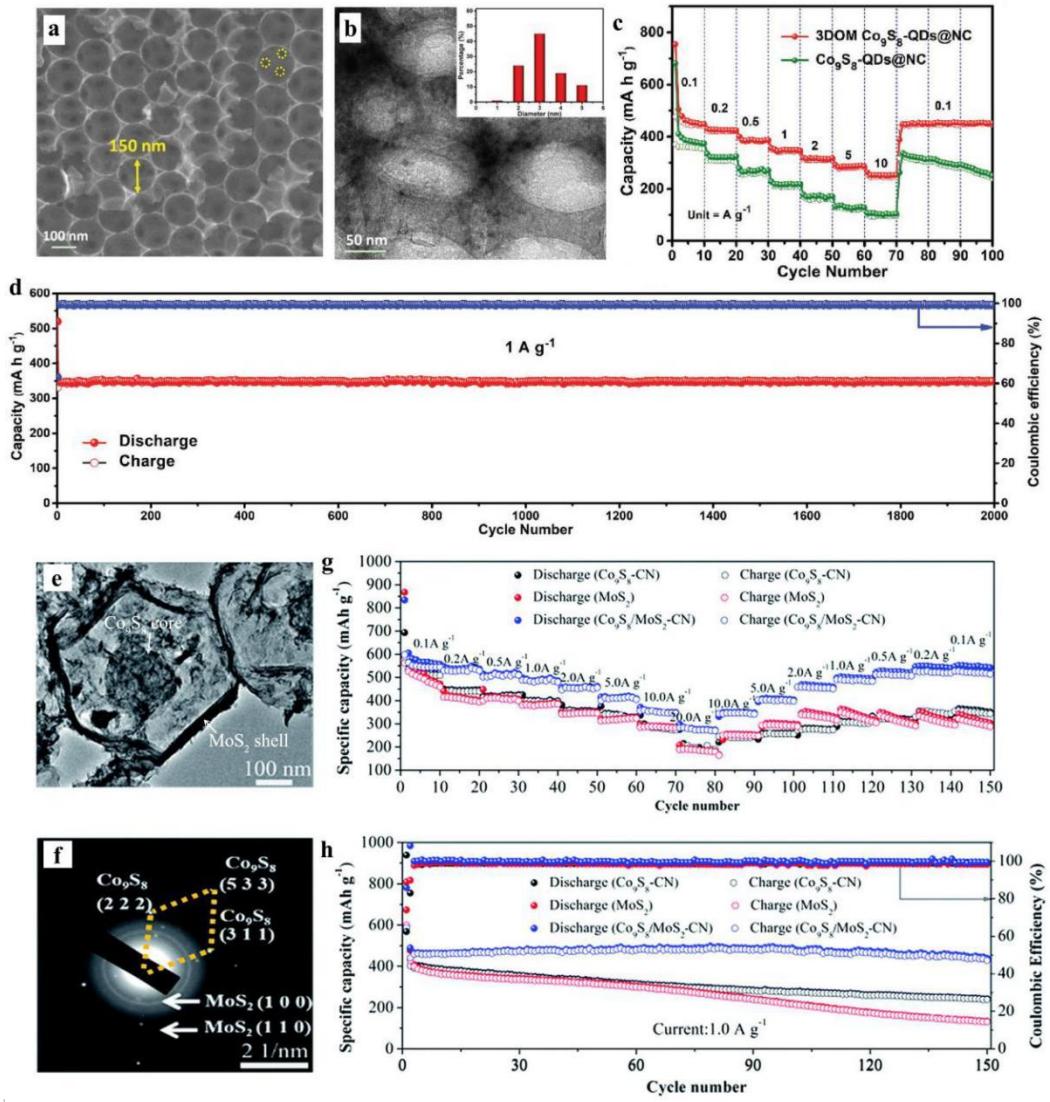


Fig. 5 (a) FESEM images and (b) TEM images with inset of the size distribution of the QDs for 3DOM Co_9S_8-QDs@NC. (c) Rate capability of the 3DOM Co_9S_8-QDs@NC and Co_9S_8-QDs@NC electrode. (d) Cycling performance and Coulombic efficiency of 3DOM Co_9S_8-QDs@NC for 2000 cycles at the current density of 1 A g^{-1}.[99] (e) TEM images and (f) SAED patterns of the yolk-shelled polyhedral Co_9S_8/MoS_2-CN nanocomposite. (g) Rate capability at different current densities and (h) cycling performance at 1.0 A g^{-1} for the Co_9S_8/MoS_2-CN composite, Co_9S_8-CN and MoS_2 anodes.[103]

ACCEPTED MANUSCRIPT

3.2 CoS_2

CoS_2 has the same crystal structure as FeS_2, which is called a pyrite phase. The schematic representation of the CoS_2 crystal structure is displayed in Fig 6.[104] A Co atom occupies the central site of an octahedral arrangement with S atoms occupying the corner site the neighboring octahedrons share corners with each other. Besides, CoS_2 is assigned to a cubic phase with the *Pa*-3 space group.

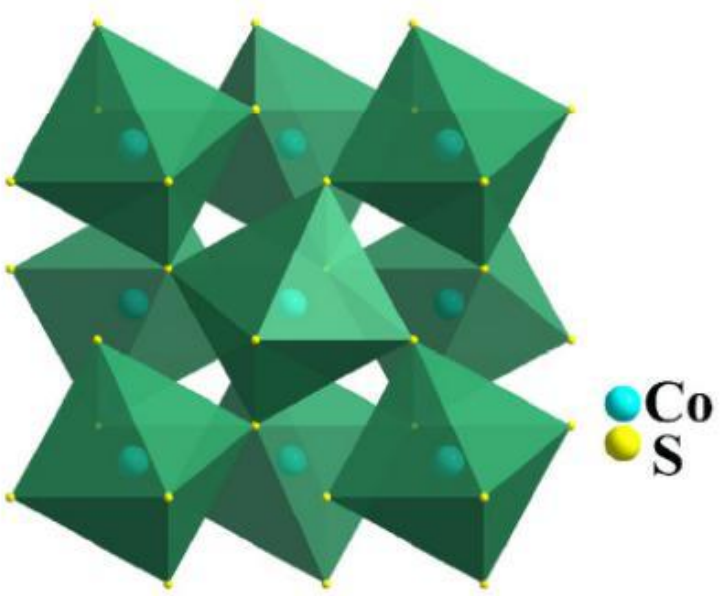


Fig. 6 Crystal structure of CoS_2.[104]

As a promising anode material for SIBs, CoS_2 offers a large theoretical capacity of 870 mAh g^{-1} and high electronic conductivity.[105, 106] The band gap of CoS_2 is 0 eV, which means this material possesses metallic-like conductivity. According to previous work,[107] as can be seen in Fig 7, each CoS_2 can react with four Na^+ ions and this electrochemical reaction can be divided into 2 steps. Firstly, when the voltage is above 1 V (*vs*. Na^+/Na), no more than two Na^+ ions inserted into CoS_2 and an intermediate product is formed. Then, with the electrochemical reaction proceeding, Co^{4+} is reduced to metallic Co and Na_2S emerged below 1 V (*vs*. Na^+/Na). The sluggish kinetics, low reversibility and huge volume change for conversion reaction that takes place in the low voltage range, causes inferior cycling performance. To solve this problem is one of the key issues for CoS_2 as an anode material for sodium ion battery.[108]

ACCEPTED MANUSCRIPT

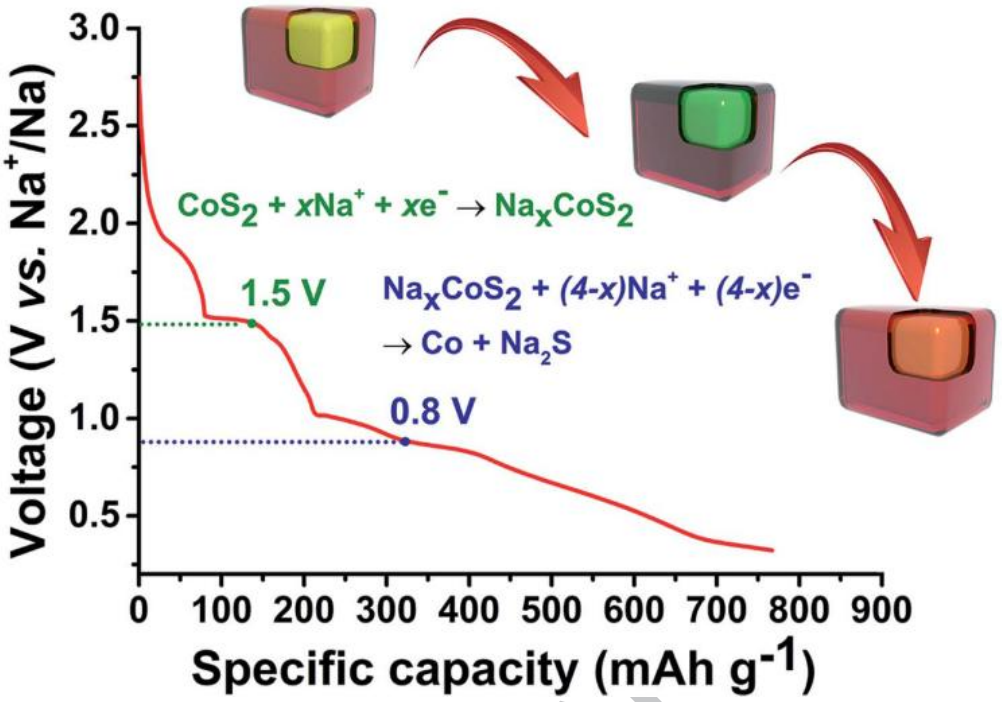


Fig. 7 Reaction mechanisms of CoS_2 in the fully discharged process.[107]

Carbon matrices or coating layers can buffer the volume change of CoS_2 during intercalation-deintercalation of Na^+ ions and associated reaction phases. Previous work has tried to introduce carbon-based materials to obtain a CoS_2-based composite with good electrochemical performance.[109-111] A kind of flower-like N-doped carbon/CoS_2 spheres (N-C/CoS_2) was synthesized by a solvothermal method followed by sulfurization.[112] As can be seen in Fig 8a, the CoS_2 flowers consist of 2D wrinkled CoS_2 nanosheets with an average thickness less than 5 nm. This open nanostructure can shorten the Na^+ ion diffusion distance in the CoS_2 crystal in principle. Combined with the carbon matrix, this composite shows a stable cycling life over 500 cycles without obvious capacity decay. In contrast, bare CoS_2 loses most of its capacity after 200 cycles. In another work, combining the template, electrospinning and solvothermal methods, a double-morphology CoS_2-N doped carbon fiber composite was synthesized.[113] As can be seen in Figure 8c, CoS_2 nanosheets were *in situ* formed on the surface of the carbon fiber. Meanwhile, CoS_2 nanoparticles also grew in the channels of these carbon fibers. This form of carbon fiber, with unique its structure, plays the dual role of matrix and coating for CoS_2 nanosheets and nanoparticles, respectively. At 0.1 A g^{-1}, this composite exhibits a high initial discharge capacity of 849.6 mAh g^{-1}, and maintains capacities of more than 700 mAh g^{-1} over subsequent cycles. In

ACCEPTED MANUSCRIPT

addition, compared with the bare CoS_2 electrode, double-morphology CoS_2-N doped carbon fiber composite demonstrate a more stable long-term cycling over 900 cycles.

Similar to Co_9S_8, heterostructures consisting of CoS_2 and other metal sulfides have also been reported.[114] SnS_2@CoS_2-rGO (reduced graphene oxide) composite shows quite a high discharge capacity and better cycling performance than SnS_2-rGO and CoS_2-rGO composites.[115] It is believed that a synergetic effect exists between CoS_2 and SnS_2, which can offer an optimal electrode/electrolyte interface. Using Prussian blue analogues, potassium hexacyanocobaltate as a precursor, a type of NiS_2@CoS_2@C@C nanocube was obtained.[116] This material also shows a stable cycling life, with more than 600 mAh g^{-1} capacity obtained after 250 cycles, at a current density of 1 A g^{-1}.

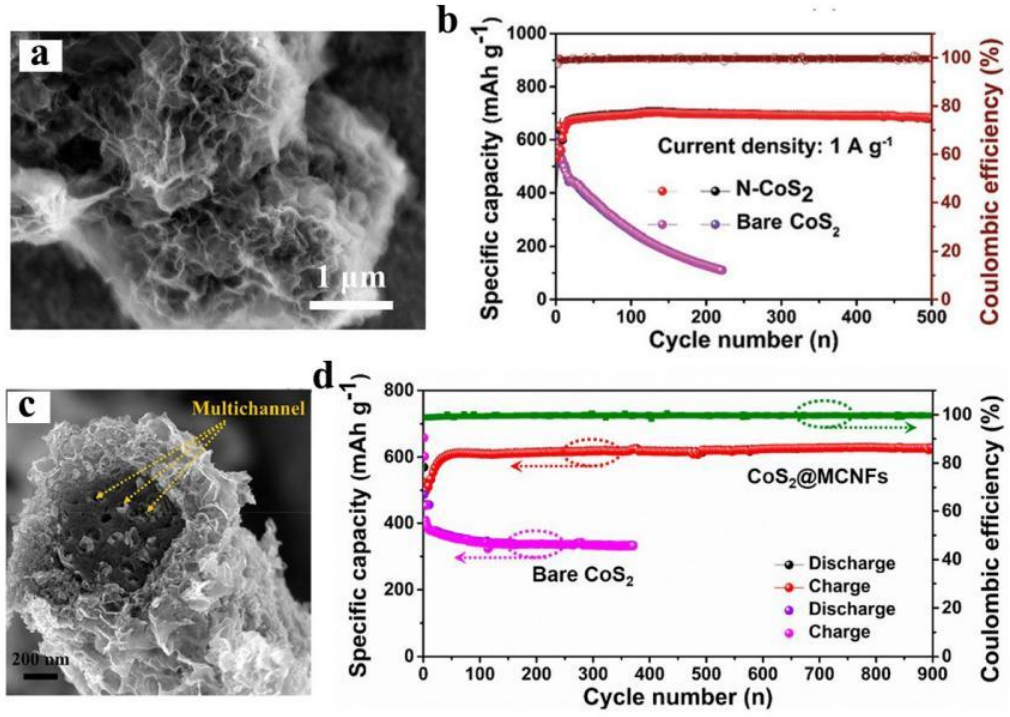


Fig. 8 (a) SEM images of the N-C/CoS_2 composites. (b) Cycling performance of N-C/CoS_2 and the bare CoS_2 electrodes at 1 A g^{-1}.[112] (c) High magnification SEM images of the CoS_2@MCNFs composites. (d) Cycling life testing of CoS_2@MCNFs electrode and bare CoS_2 electrode.[113]

It has been pointed out that when using ether-based electrolyte, CoS_2-based electrodes show both better cycling stability and rate capability, than with carbonate-based electrolyte.[117] Several factors causing this better performance have been proven, with some mechanistic

ACCEPTED MANUSCRIPT

similarities for Li-S systems. Firstly, a more stable SEI membrane can form in ether-based electrolyte, which means less consumption of electrolyte and sodium salt. Then, ether-based electrolytes have a better wettability with electrodes than carbonate-based electrolytes. Finally, faster charge-transfer kinetics can be observed in ether-based electrolytes.

3.3 CoS

CoS is another type of cobalt chalcogenide, which has been regarded as another potential anode material for the alkaline ion battery.[118] It appears that almost all of the CoS investigated within the energy storage field is indexed to the hexagonal crystal phase with a *P63*/mmc space group. The corresponding crystal structure is shown in Fig 9.[119] Every crystal cell possesses two Co^{2+} ions and S^{2-} ions. Each Co^{2+} ion occupies the center site of octahedron with six S^{2-} ions coordinate it; the adjacent CoS_6 octahedrons share edges and faces. As an anode material for sodium ion battery, CoS has a theoretical capacity of 588 mAh g^{-1}. In a Na^+ ion intercalation process, each CoS will react with two Na^+ ions. Similarly with CoS_2, this reaction can be divided into two steps, the insertion step ($CoS + xNa^+ + xe^- \rightarrow Na_xCoS$, $x<2$) and the conversion step ($Na_xCoS + (2-x)Na^+ + (2-x)e^- \rightarrow Co + Na_2S$). Generally, the conversion step takes place below 0.8 V.[120-122]

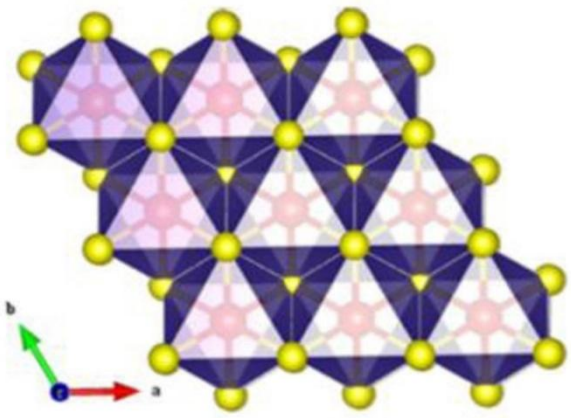


Fig. 9 Crystal structure of hexagonal CoS.[119]

It is well known that the conversion reaction faces similar challenges to other materials discussed previously such as volume expansion, low reversibility and so on.[123-128] Thus, there is no doubt that the conversion step has a remarkable influence upon the electrochemical

ACCEPTED MANUSCRIPT

performance of CoS. As can be seen in Fig. 10b,[123] when the potential window is extended to 0.1-2.9 V, allowing the conversion step to dominate, more than 75% of initial capacity decayed after 500 cycles at 1 A g^{-1}. In contrast, when the cut-off voltage was set to 0.6 V to avoid the conversion step, as shown in Fig. 10a, a high retention rate of 88% could be obtained over 1000 cycles at the same current density. However, although this potential window controlling strategy is highly effective, the capacity provided by conversion step will not be provided. Finally, if the CoS electrode is assembled in a full cell system, the overall reduction of the energy density within this device, will not provide a suitable energy storage platform. Thus, there is a vast requirement to develop methodologies that will alleviate the problems caused by the conversion step.

A method to overcome this destructive conversion step is to use a Co based MOF as a precursor to build porous carbon substrate. For example, through a facile calcination method within inert gas, CoS nanoparticles embedded into porous carbon rods were synthesized by Zhou et al.[119] In the optimized sample, the average size of CoS particles was 7 nm (7-CoS/C). This ultrathin particle suffered more expansion stress than the larger particles with average size of 18.5 nm (18.5-CoS/C). As displayed in Fig. 10c, the composite electrode consisting of 7 nm-sized CoS particles exhibits an improved cycling life than that those containing larger sized active material particles. Additionally, a smaller particle size can also shorten Na^+ ion diffusion path leading to an increased rate capability. These approaches confirm that the conductive host is important to alleviate increased material resistance from smaller particles with similar tap density to electrode formulations with larger particles, while nanoscaling ensures a better tolerance to volume expansion and accommodation of conversion mode products during cycling.

ACCEPTED MANUSCRIPT

ACCEPTED MANUSCRIPT

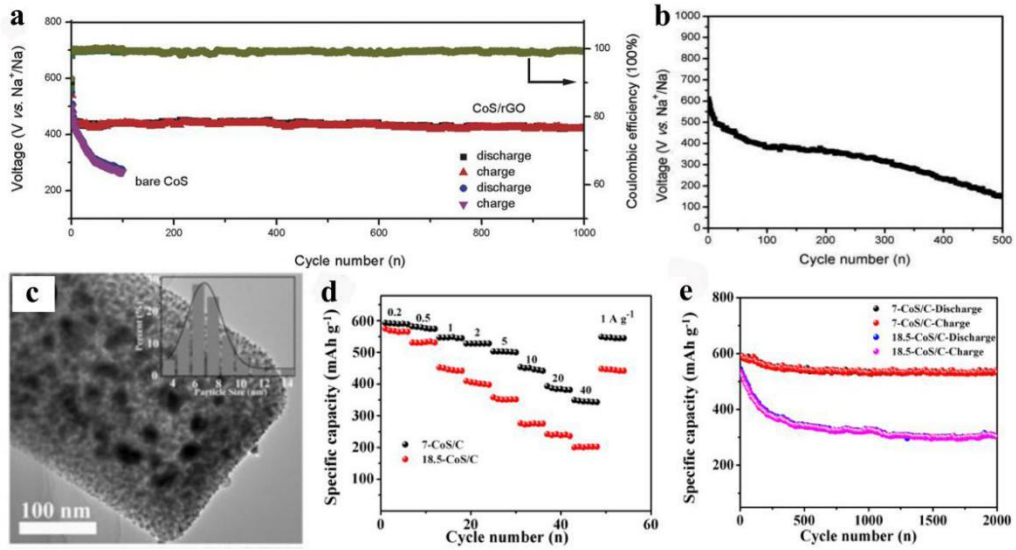


Fig. 10 (a) Cycling performance (left) and Coulombic efficiency (right) of the CoS@rGO composite at a current density of 1 A g^{-1} over a voltage window of 0.6-3.0 V. (b) Cycling performance of CoS/rGO at a current density of 1 A g^{-1} over a potential window of 0.01-2.9 V.[114] (c) High-resolution TEM with inset of particle size distribution diagram for 7-CoS/C. (d) Rate capability and (e) cycling performance at a current density of 1 A g^{-1} in the voltage range of 0.6-3 V (*vs*. Na^+/Na) for 7-CoS/C and 18.5-CoS/C electrodes.[119]

The construction of a yolk-shell structure can also address the aforementioned problems. Recently, Mai's group reported a self-adaptive CoS@C with yolk-shell microsphere composite was obtained by SiO_2-templated method.[129] Briefly, as shown in Fig. 11a, the silica and resorcinol formaldehyde (RF) was coated on the CoS precursor. After an annealing process, the resulting SiO_2 particles were etched by HF and the yolk-shell structure was obtained. The resulting morphologies of the cycled samples were also investigated. The CoS micron spheres without carbon shells deteriorated after 10 cycles and were totally pulverized after 50 cycles. Nonetheless, the yolk-shell CoS@C composite can maintain its structural integrity even after 50 cycles. The gap-space was states as the reasons why this material could accommodate the volume expansion of the products during the conversion step (Co and Na_2S), with the carbon shell preventing the loss of active material.

ACCEPTED MANUSCRIPT

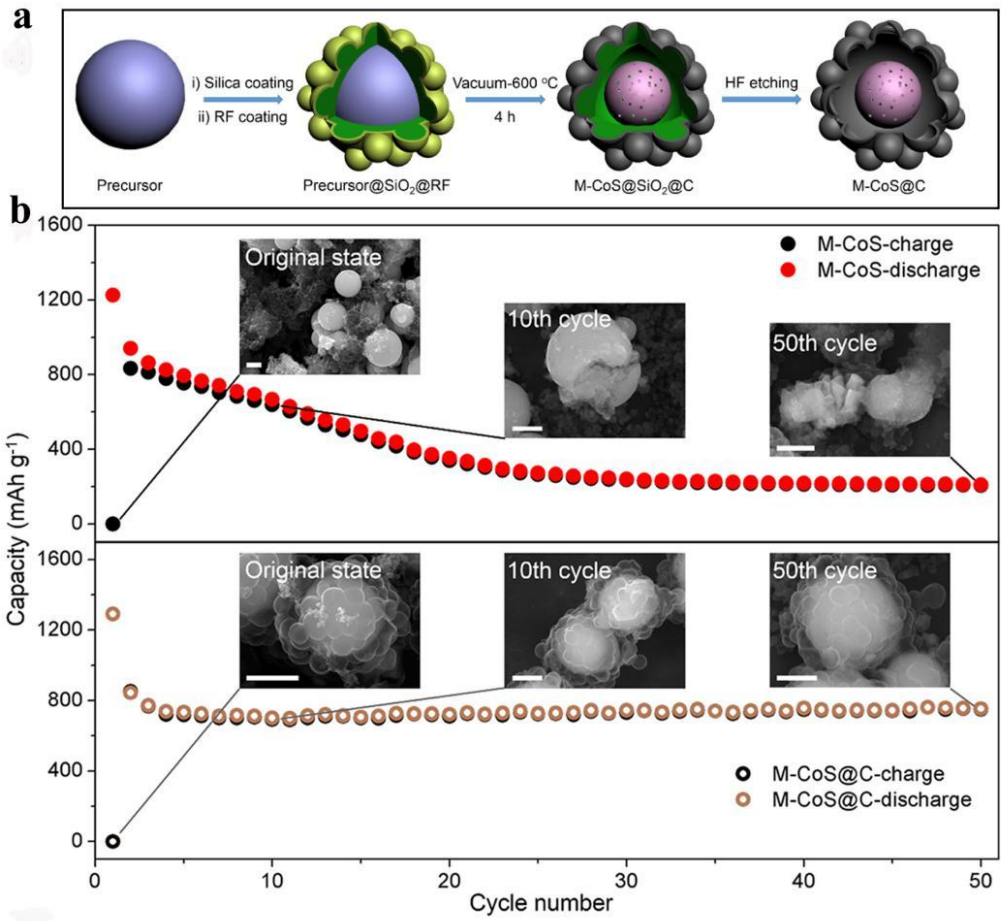


Fig. 11 (a) Schematic illustration of the synthesis of yolk-shell M-CoS@C. (b) The SEM images of the M-CoS and yolk-shell M-CoS@C at 0, 10th and 50th cycle (full charge state) respectively, and their corresponding cycling performances at 1 A g^{-1}. Scale bar, 1 μm.[129]

4. Cobalt Selenide Anodes

4.1 $CoSe_2$

Generally, compared with other metal oxides and sulfides, metal selenides possess higher volumetric capacity and electrical conductivity, and have been routinely applied within SIBs.[130, 131] Generally, metal selenides have similar properties with metal sulfides, resulting in the wide range of investigations of $CoSe_2$, as a promising anode for SIBs. $CoSe_2$ has two different phases, namely the trogtalite and hastite phases. The first belongs to an orthorhombic marcasite phase with a space group of *Pnnm* and the second is the cubic phase with a space group of *Pa3*. Both of these phases of $CoSe_2$ have been studied as anode materials for SIBs.[132, 133] For example, the crystal structure of hastite phase is shown in Figure 12a, and, six Se anions coordinate to a Co^{2+}

ACCEPTED MANUSCRIPT

ion, which occupies the center site of the octahedron. The adjacent Se anions forms a Se_2^{2-} anion via a covalent Se-Se bond.[132]

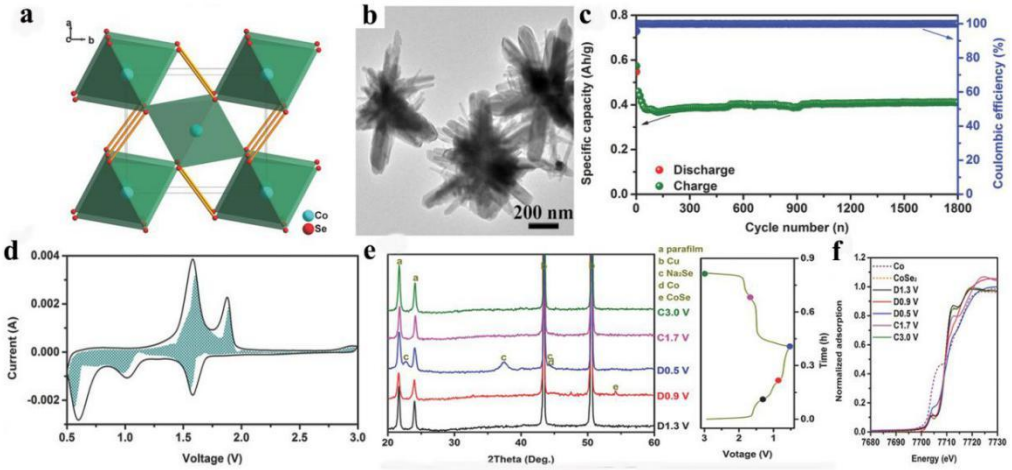


Fig. 12 (a) Crystal structure of the marcasite-type $CoSe_2$. (b) TEM and (c) cycling life of the $CoSe_2$ at a current rate of 1 A g^{-1}. CV curve with the pseudocapacitive fraction shown by the darkly cyan region at a scan rate of 1 mV s^{-1}. (e) Reaction mechanism: *ex situ* XRD analysis of the $CoSe_2$ electrodes at different charge-discharge states with the corresponding charge-discharge curve and parafilm was used to protect the $CoSe_2$ electrodes when testing XRD. (f) Near-edge X-ray absorption spectroscopy of the $CoSe_2$ electrodes at different cycling states and the reference Co and $CoSe_2$.[132]

Ou and co-workers focused on the mechanism for Na^+ ion intercalation reaction with $CoSe_2$. It has been proven that this electrochemical reaction can be divided into three steps and CoSe forms as an intermediate product. In detail, the three steps are as follows[134]:

Intercalation step: $CoSe_2 + xNa^+ + xe^- \rightarrow Na_xCoSe_2$ (x<2, >1.0 V)

Transition step: $Na_xCoSe_2 + (2\text{-}x)Na^+ + (2\text{-}x)e^- \rightarrow Na_2Se + CoSe$ (1.0-0.8 V)

Conversion step: $CoSe + yNa^+ + ye^- \rightarrow Na_2Se + Co^0$ (0.8-0.01 V)

Based upon this electrochemical reaction with four electrons, $CoSe_2$ exhibits a theoretical capacity of 494 mAh g^{-1}. However, as with CoS_2, the application of $CoSe_2$ is hindered by its poor cycling performance due to the volume change and structural pulverization[135, 136].

Chen's group synthesized a kind of urchin-like $CoSe_2$, which consists of multiple nanorods as

ACCEPTED MANUSCRIPT

shown in Fig. 12b,[132] with pseudocapacitive behaviors (Fig. 12d) that can lead to a stable cycling life. This material shows a high reversible capacity of 410 mAh g^{-1} after 1800 cycles, at a current density of 1 A g^{-1}, over a potential window of 0.5-3.0 V as displayed in Fig. 12c. Upon incorporation into a $Na_3V_2(PO_4)_3/CoSe_2$ full cell, the urchin-like $CoSe_2$ still exhibits a high capacity of 380 mAh g^{-1}. However, there is a huge capacity loss between the 1st and 2nd cycles, which could be due to the irreversible formation of SEI. To further understand this phenomenon, as exhibited in Fig. 12e-f, *ex situ* XRD analysis and near-edge X-ray absorption spectroscopy determined that, after the first discharge process, even upon charging to 3.0 V, the anode material did not return to its original pristine state, as some Na^+ ions were not extracted from the anode material. Thus, upon subsequent cycles, the reversible electrochemical reaction starts and ends with the state of Na_xCoSe_2, which unavoidably hinders the capacity of the anode material.

Another methodology that has been considered is the synthesis of a novel type of $CoSe_2$@C bridged with carbon nanotubes ($CoSe_2$@C/CNTs) reported by Qiu et al.[136] As can be seen in Fig 13, the precursor, ZIF 67, was annealed in H_2/Ar mixed gas and the Co^{2+} was reduced to form Co metallic nanoparticles. These metal particulates act as a catalyst promoting the formation of the carbon nanotubes. In this hierarchical structure, the CNT can construct a cross-linked conductive network and prevent the agglomeration of the active material. This composite demonstrates a high reversible specific capacity of about 470 mAh g^{-1} at a current density of 0.2 A g^{-1}. After 1000 cycles, a superior capacity retention closing to 100% can be observed (calculated from the 70th cycles).

ACCEPTED MANUSCRIPT

ACCEPTED MANUSCRIPT

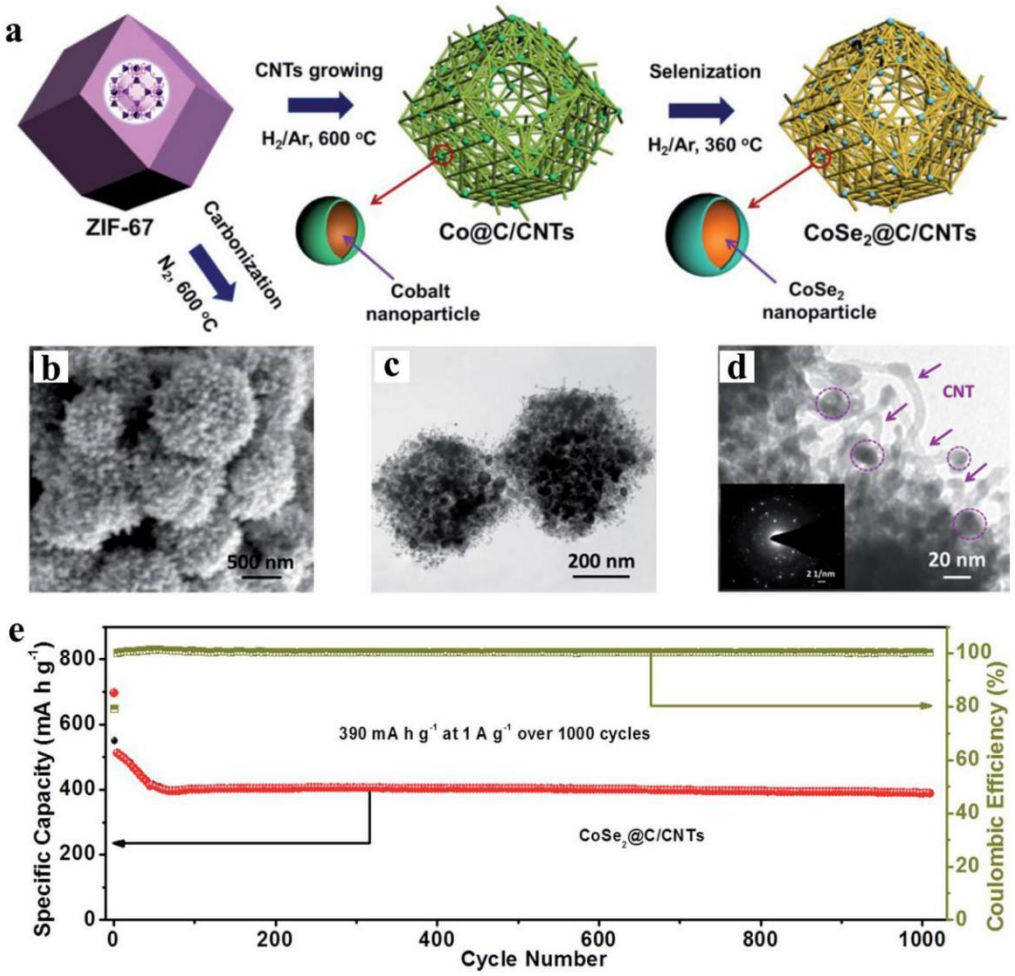


Fig. 13 (a) Synthetic processes of the $CoSe_2$@C/CNTs and $CoSe_2$@GC. (b) FESEM images and (c) TEM images exhibiting the polyhedral $CoSe_2$@C/CNTs integrated with tangled CNTs and carbon-coated $CoSe_2$ nanospheres; (d) TEM image of the CNTs (shown by purple arrows) on $CoSe_2$ particle surface; the SEAD patterns (inset) suggest the polycrystalline structure of $CoSe_2$ nanospheres in the hybrid. (e) Long-life cyclability of the $CoSe_2$@C/CNTs anode.[136]

The structural design of coating other kind of metal sulfides to form heterostructure has been also applied for optimizing the electrochemical performance of $CoSe_2$.[137, 138] Through a facile synthesis route combining hydrothermal coating and selenization processes, $CoSe_2$ particles with $MoSe_2$/C shells were developed as a composite ($CoSe_2 \subset MoSe_2$/C).[139] This $MoSe_2$/C hybrid shell was reported to simultaneously enhance the transition of both ions and electrons, alleviating the volume change during alkaline ion insertion/extraction processes. Combining this with a capacitive contribution, this composite shows a specific capacity of 450 mAh g^{-1} over 100 cycles

ACCEPTED MANUSCRIPT

at 0.1 A g^{-1}, and maintains more than 300 mAh g^{-1} capacity at 1 A g^{-1} after 200 cycles, respectively.

4.2 Other cobalt selenides

Recently, Chen's group reported the utilization of porous $Co_{0.85}Se$ ultrathin nanosheets anchoring on rGO composite as an anode for SIB. The morphology of as prepared $Co_{0.85}Se$ nanosheets is shown in Fig 14a.[140] As can be seen in Fig. 14b-c, this composite shows superior capability and stable cycling life over 800 cycles at 1 A g^{-1}. This hierarchical nanostructure can provide enough active sites for Na^+ ions adsorption and reserve space to accommodate the volume change. Importantly, the unequal content of Co and Se elements in $Co_{0.85}Se$ leads to the formation of defects. As shown in Fig. 14d-e, the band gap calculation by using density function theory (DFT), shows that the $Co_{0.85}Se$ has a narrower band gap (0.68 eV) than that of the CoSe (1.36 eV), meaning an enhanced electronic conductivity. These defects also provide suitable Na^+ ion diffusion pathways, which can lead to a lower migration energy barrier of $Co_{0.85}Se$ than for CoSe as displayed in Fig. f-g, respectively. Additionally, the possible Na^+ ion diffusion trajectories in above two kinds of materiovals are shown in Fig. 14h. The bond length of Co-Se in $Co_{0.85}Se$ is longer than that in CoSe, leading to faster reaction kinetics for the $Co_{0.85}Se$ conversion to Co and Na_2Se.

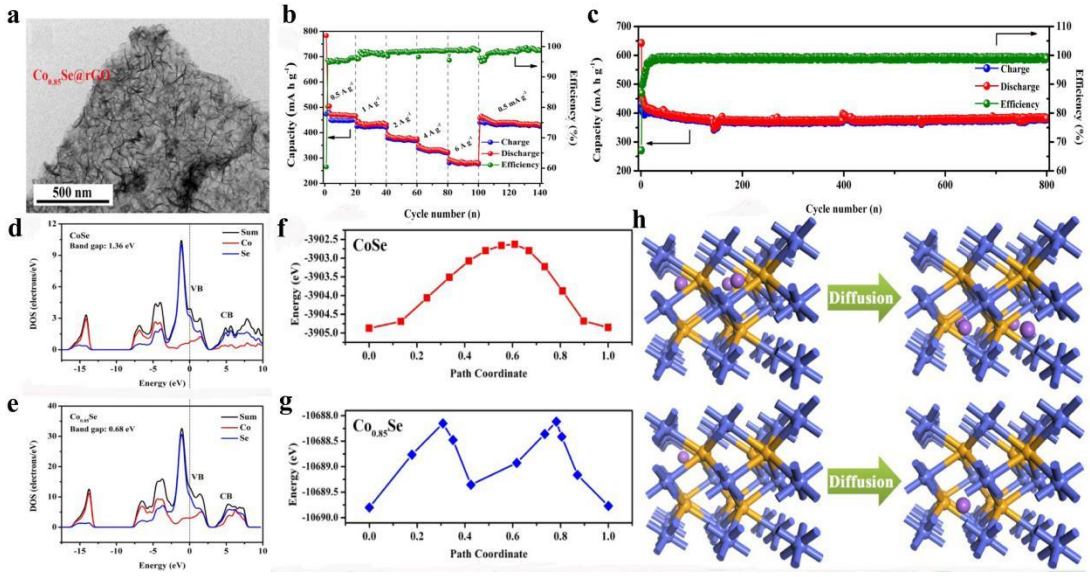


Fig. 14 (a) TEM images of $Co_{0.85}Se$ NSs@rGO. (b) Rate performance at different current densities and (c) long-cycling performance at 1 A g^{-1} for $Co_{0.85}Se$ NSs@rGO electrode. (d-e) DOS and

ACCEPTED MANUSCRIPT

PDOS spectra of CoSe and $Co_{0.85}Se$. (f-g) The calculated migration energy barriers of the single Na^+ ions along the described paths. (h) Possible Na^+ ion diffusion trajectories in CoSe (upper schematics) and $Co_{0.85}Se$ (lower schematics) through the vacancy site.[140]

Another $Co_{0.85}Se$/graphene composite has been reported by Zhou's group, as a binder-free anode electrode for alkaline ion battery.[141] As can be seen in Figure 15, the $Co_{0.85}Se$ nanosheets anchored on graphene stably and this "sheet-on-sheet" nanostructure with strong interfacial interaction can self-assemble to form a flexible film electrode without any conductive additive and binder. It is believed that the strong interfacial interaction between different parts of the composite can effectively enhance the electron transfer. Graphene can not only play a role of conductive matrix, but also protect the $Co_{0.85}Se$ from agglomeration after the charge-discharge test. Besides this, the binder-free strategy can improve the volumetric specific capacity of this electrode. When applied to SIBs, this novel electrode exhibits a preferred stable cycling performance and better rate capability than pure $Co_{0.85}Se$ nanosheet electrode.

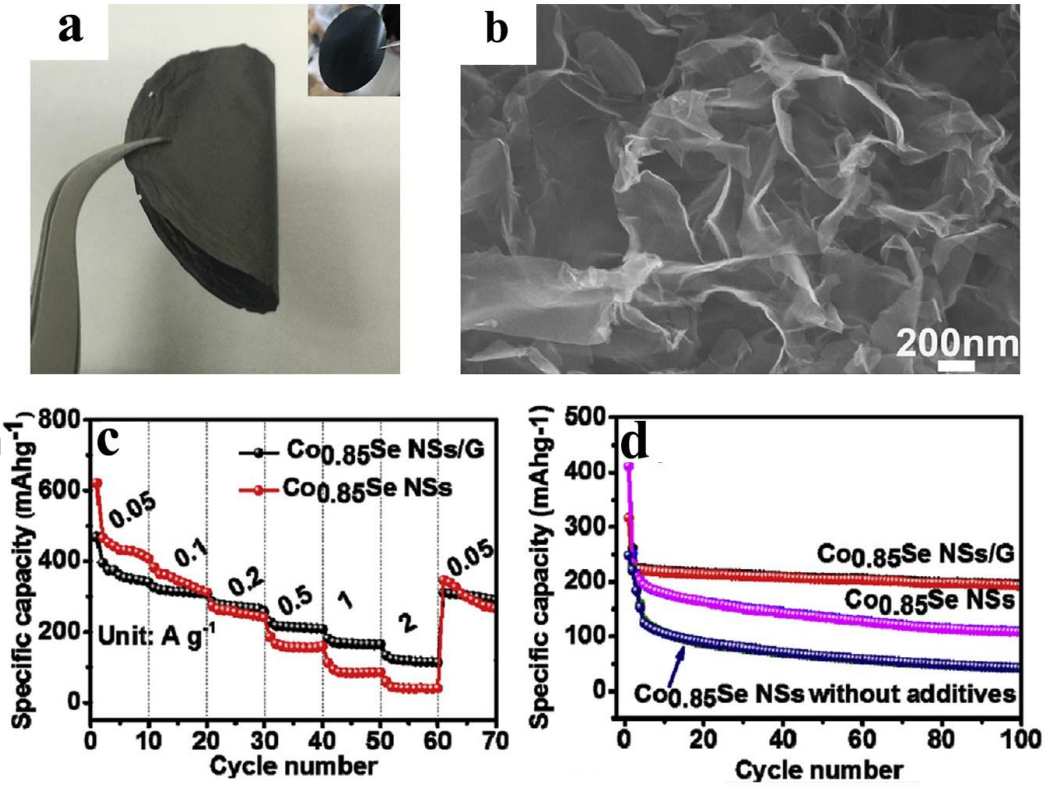


Fig. 15 (a) Optical images of the $Co_{0.85}Se$ NSs/G film with the inset of $Co_{0.85}Se$ NSs/GO film. (b) SEM images of $Co_{0.85}Se$ NSs. (c) Sodium storage rate performance of the $Co_{0.85}Se$ NSs and the

ACCEPTED MANUSCRIPT

$Co_{0.85}Se$ NSs/G film. (d) Cyclic properties of the $Co_{0.85}Se$ NSs with and without the addition of a binder and conducting additives and of the $Co_{0.85}Se$/G film at a current density of 0.5 A g^{-1}.[141]

CoSe is another kind of cobalt selenide material which has been used as anode material for SIBs. Like other cobalt chalcognides, CoSe possesses a remarkable electrical conductivity and suffers from terrible volume expansion. Besides, compared with other cobalt chalcognide anode, the theoretical capacity of CoSe is relatively lower, no more than 390 mAh g^{-1}.[121] However, this capacity is higher than the capacities of most carbon-based anode for SIBs. Therefore, CoSe, as anode material for SIBs, has attracted some research attention so far.[142, 143] The electrochemical reaction of CoSe occurs as follow[144]:

$$CoSe + 2Na^+ + 2e^- \rightleftharpoons Co + Na_2Se$$

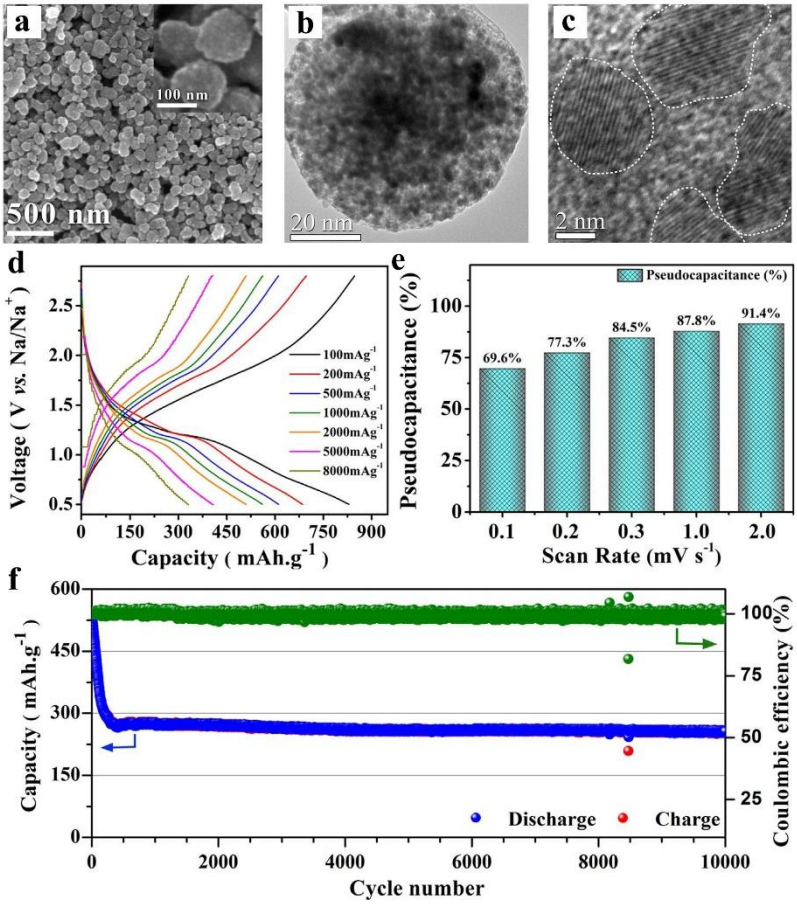


Fig. 16 (a) SEM image, (b) low and (e) high magnification TEM images of CoSe@carbon spheres (CoSe@CSs). (d) charging-discharging curves at different current densities (e) the pseudocapacitive charge storage contribution (in percentage) at different scan rates and (f) long-term cycling performance in the voltage range of 0.5-2.8 V with 4000 mA g^{-1} current density

ACCEPTED MANUSCRIPT

of CoSe@CSs electrode.[145]

To address the volume expansion issue, CoSe always has been designed to nano-structure and combined with carbon matrix. Hou's group synthesized a CoSe embedded in carbon spheres composite (CoSe@CSs).[145] As displayed in Fig. 16a, the average diameter of this composite is about 100 nm. TEM images (Fig. 16b-16c) show that a single composite sphere is made of many CoSe nanoparticles and a carbon matrix. The sizes of such CoSe nanoparticles are about 3 nm to 10nm. As can be seen in Fig. 16d, CoSe@CSs composite shows good rate capability. In detail, at 8000 mA g^{-1}, a high discharging capacity of 222 mAh g^{-1} still retained. This good rate capability can be attributed to two main reasons. Firstly, the carbon sphere plays a role of conductivity substrate. Secondly, the pseudocapacitive behaviors also enhance the rate performance. As shown in Fig. 16e, with the scan rates increased, more and more electrochemical behavior became capacitive controlled. At 2 mV s^{-1}, the pseudocapacitive charge-storage amount occupies a high portion of more than 90% of the whole capacity. Besides, the carbon matrix can also buffer the volume expansion during sodiation/desodiation reactions. As a result, this CoSe@CSs shows an outstanding cycling performance. A capacity of 260 mAh g^{-1} can be reserved at 4000 mA g^{-1} even after 10000 cycles (Fig. 16f).

5. Cobalt Phosphide Anodes

Transition-metal phosphides (TMPs) is a kind of popular material for hydrodesulfurization, water electrolysis, dehydrogenation of borohydrides, fuel cell and electrochemical energy storage applications.[146] Among these TMPs, CoP has been considered as a promising anode material for SIBs for its high electrical conductivity and large theoretical specific capacity of 890 mAh g^{-1}.[147, 148] The sodium storage reaction is present as follows[149]:

$$CoP + 3Na^{+} + 3e^{-} \rightleftharpoons Co + Na_3P$$

However, unoptimized CoP material always shows an unsatisfying Na ion storage performance. There are two problems which can be to blame for it. The first one is the extremely huge volume expansion, which is closed to 500%, during the sodiation/desodiation process. This will lead to pulverization of the electrode material. The second one is the side reaction during charging process. This side reaction can be present as follows[150]:

ACCEPTED MANUSCRIPT

$$Na_3P \rightleftharpoons P + 3Na^+ + 3e^-$$

Li and co-workers analysed the material composition of CoP electrode after charged to 3 V by ex situ XRD and ex situ TEM.[149] The signal of metal Co phase could be detected. This result suggests that some P did not react with Co to form CoP. Metal Co cannot react with Na^+ ion and pure P has a low electrical conductivity (about 10^{-14} S cm^{-1}). To obtain better Na^+ ion storage performance, to improve the structural stability of CoP electrode is necessary.

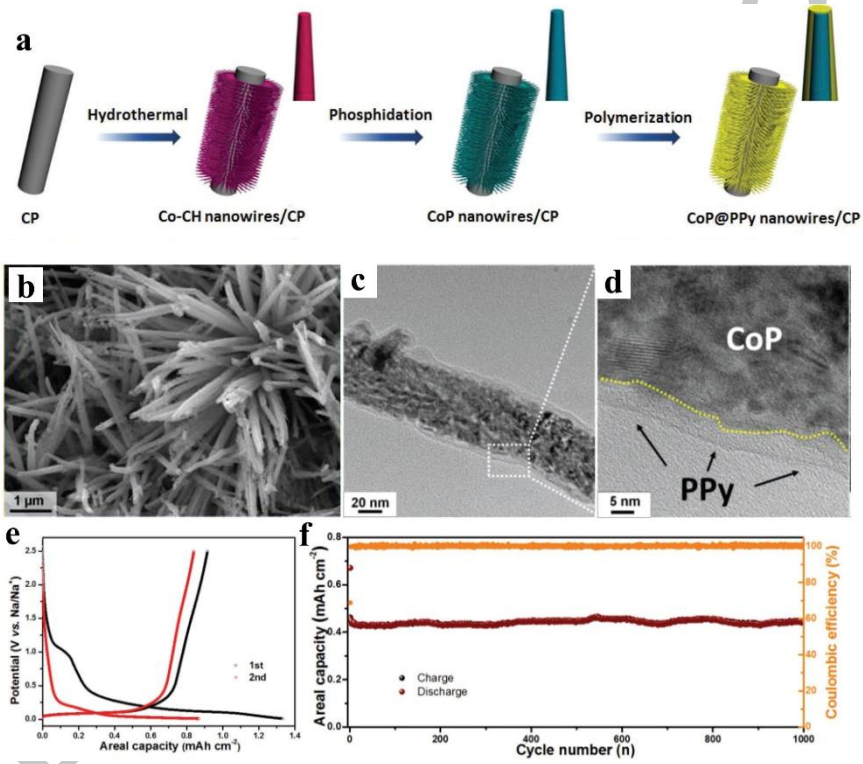


Fig. 17 (a) Schematic diagram of the fabrication process for CoP@polypyrrole nanowires/carbon paper electrode (CoP@PPy nanowires/CP electrode). (b) SEM images, (c) TEM images and (d) HRTEM image of CoP@PPy NWs/CP. (e) Charge-discharge curves for the first two cycles at 0.15 mA cm^{-2} and (f) Long-term cycling stability at 1.5 mA cm^{-2} of the CoP@PPy NWs/CP electrode.[151]

To introduce polymers and carbon material as coating layer or flexible substrate are the most common strategies to improve the structure stability of CoP electrode. Kang's group utilized the carbon paper (CP) as the substrate and grew cobalt carbonate hydroxide hydrate ($Co(CO_3)_{0.5}OH{\cdot}0.11H_2O$, notated as Co-CH) nanowires on it. Then, after a phosphidation process,

ACCEPTED MANUSCRIPT

CoP nanowires formed. At last, the polypyrrole layer was in situ formed through a facile polymerization reaction.[151] The schematic diagram of the above-mentioned process is shown in Fig. 17. Fig. 17b shows the polypyrrole coated CoP wires. As can be seen in Fig. 17c-17d, the diameter of this kind of nanowire is about 50 nm and the thickness of polypyrrole layer is about 5 nm. On one hand, the CP can serve as a conductive substrate. On the other hand, the polypyrrole coating layer can buffer the volume change effectively to prevent the morphology pulverization. As a result, this CoP@PPy nanowires/CP composite shows good Na^+ ion storage performance as anode for SIBs. In detail, as can be seen in Fig. 17e, this electrode shows a high reversible capacity of about 0.85 mAh cm^{-2} in the second cycle. In addition, the long-term cycling stability is shown in Fig. 17f. There is no obvious capacity decay over 1000 cycles.

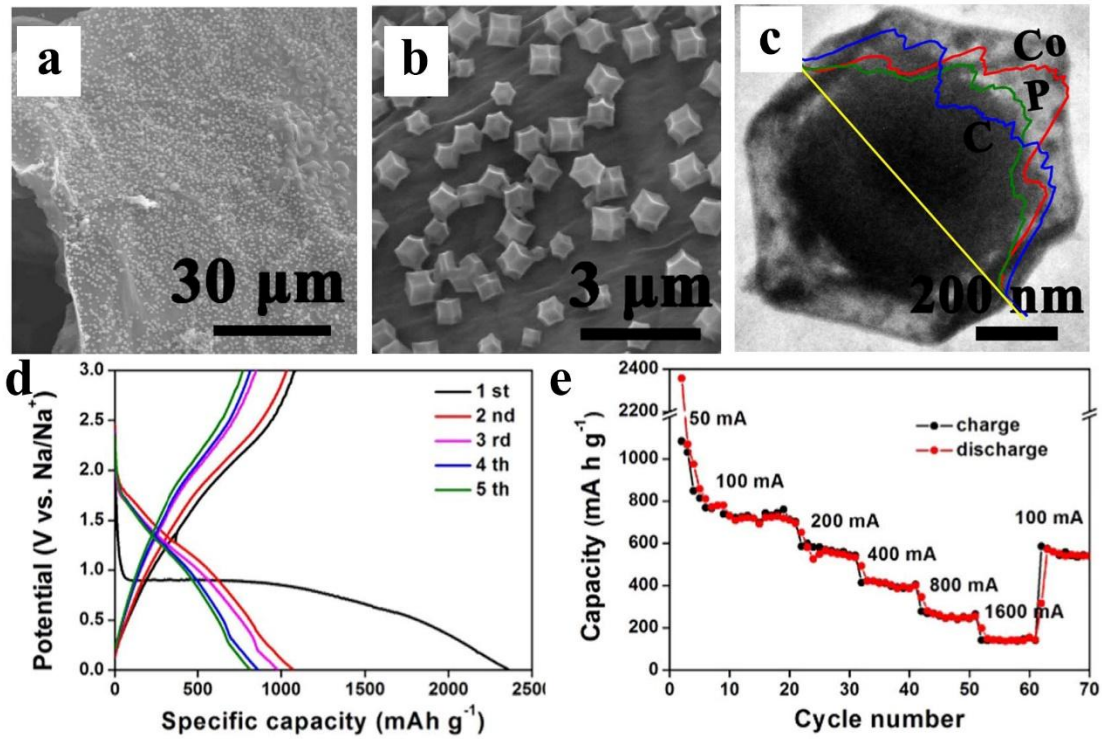


Fig. 18 (a-b) SEM images of CoP@C-reduced graphene oxide-nickel foam composite (CoP@C-RGO-NF). (c) TEM image of a single CoP@C polyhedron, the inset is line scanning curves of elemental distribution of CoP@C. (d) Galvanostatic charging/discharging curves at a current density of 50 mA g^{-1} for first two cycles and 100 mA g^{-1} for last three cycles and (e) rate capability of CoP@C-RGO-NF electrode.[152]

ACCEPTED MANUSCRIPT

Another common strategy to obtain good Na^+ ion storage performance of CoP electrode is using ZIF-67 as precursor. Generally, this precursor can bring the advantages of uniform and nano-sized particle size. And the organic framework can convert to conductive carbon framework by a carbonization process. Yin and co-workers synthesized a type of CoP@C-RGO-NF electrode from the ZIF-67 precursor.[152] As shown in Fig. 18a, a number of uniform CoP@C polyhedrons anchor on the surface of RGO. The size of a single CoP@C polyhedron is about 800 nm, as shown in Fig. 18b. The line scanning image in Fig. 18c exhibits that Co and P elements mainly exist at the interior section. This core-shell structure has both the high electrical conductivity and the structure stability. Benefited from this structure, CoP@C-RGO-NF composite shows good electrochemical performance as anode material for SIBs. Fig. 18d shows the charging/discharging profiles of the initial five cycle of this anode electrode. It should be noticed although the initial discharging capacity is high, there is a huge capacity decay between the first and second cycle, because of the irreversible SEI formation. In the subsequent cycles, the reversible capacity of about 1000 mAh g^{-1} can be obtained. The rate capability of CoP@C-RGO-NF electrode is shown in Fig. 18e. At the high current densities of 800 mA g^{-1} and 1600 mA g^{-1}, it can still reserve a capacity of 254 mAh g^{-1} and 155 mAh g^{-1}, respectively.

6. $Na_{0.7}CoO_2$ SIB Cathodes

Sodium cobaltates, Na_xCoO_2 ($0.5 \leq x \leq 1$), are a significant cathode material for SIBs. Researchers have paid much attention to this type material for two main reasons.[153-155] Firstly, several transition-metal oxides cathodes for SIBs, such as Na_xVO_2, Na_xCrO_2, Na_xMnO_2, several sodium cobaltates, Na_xCoO_2 ($0.5 \leq x \leq 1$), have been routinely examined for the electrochemical sodium intercalation as early as the early 1980s.[156] Secondly, the success of $LiCoO_2$ as the cathode for lithium-ion battery, also promotes research on Na_xCoO_2 for SIBs.[157]

Na_xCoO_2 has a layered structure that can be described as OCONOCON..., where the O represents oxygen, C represents cobalt and N represents sodium. According to the various sodium coordination, there are four different phases that can be identified within the sodium composition range from 0.5 to 1.[16] Following the traditional nomenclature, these four phases are denoted as O3, O′3, P′3 and P2 phases. Briefly, O is the octahedral coordination and P represents the trigonal prismatic coordination of the sodium ions; the number two (2) or three (3) implies the number of

ACCEPTED MANUSCRIPT

distinguishable sodium layers within the structure. These various phases can be obtained by controlling the sodium concentration. Specifically, $NaCoO_2$ is an O3 structure, $Na_{0.77}CoO_2$ is an O′3 structure, $Na_{0.64}\leq x\leq_{0.77}CoO_2$ is a P2 structure and $Na_{0.55}\leq x\leq_{0.6}CoO_2$ is a P′3 structure, respectively. Various crystal structures lead to differing electrochemistry and electrochemical performances. For example, the O3-phase cathode will transform into O′3 or P′3 phase. If the electrochemical reaction starts with the O′3 or P′3 phase, the value of 'x' can increase and the O3 phase material is always obtained, as shown in Fig. 19a. Many previous studies reported that the phase transition between the above three phases can easily take place at room temperature.[157, 158]

In contrast, when the electrochemical reaction starts with the P2 phases, the pristine structure can be preserved over the whole electrochemical process, as displayed in Fig. 19b.[159] Although this type of sodium cobaltate also undergoes a complex electrochemical reaction, the multiple plateaus upon charge-discharge are caused by the redistribution of Na^+ during intercalation-deintercalation process, not by the phase transitions. As a result, an improved structural stability leads to an overall better electrochemical performance. As far back as 1981, Delmas and co-workers found that the P2 phase sodium cobaltates possess the highest capacity (~ 95 mAh g^{-1}) among the different types of sodium cobaltates.[158] Besides, P2 phases offer longer cycle life and higher energy efficiency. Thus, P2 type sodium cobaltates have attracted much attention and have been regularly studied. In the following paragraphs in this section, P2 type sodium cobaltates will be discussed in detail.

ACCEPTED MANUSCRIPT

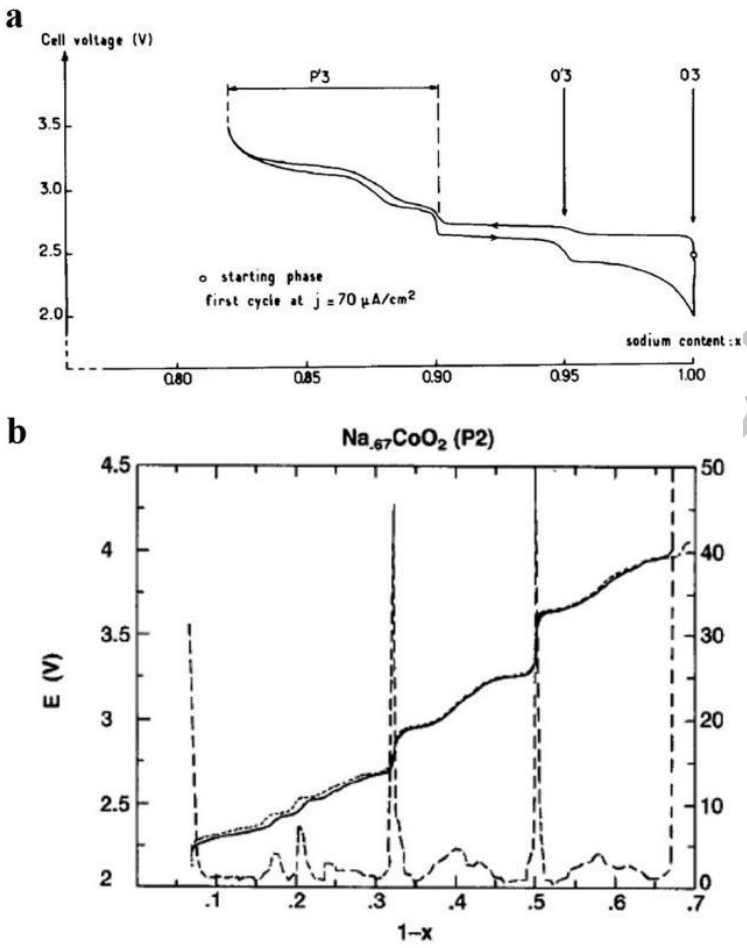


Fig. 19 (a) Emf composition curve obtained from $NaCoO_2$ (O3).[158] (b) Open-circuit potential *vs.* composition for P2-$Na_{067}CoO_2$ during ion intercalation (solid curve) and deintercalation (dotted curve).[159]

Table 1. Main characteristics of $LiCoO_2$ and P2-Na_xCoO_2

Characteristics	$LiCoO_2$[160]	P2-Na_xCoO_2
Crystal System	hexagonal	
Space Group	R3m	P63/mmc
Ion Diffusion Coefficients	0.5-1×10^{-9} cm^{-2} s^{-1} (for Li^+ ion)	0.5-1.5×10^{-11} cm^{-2} s^{-1} (for Na^+ ion)
Working Voltage	3.8 V (vs. Li/Li^+)	2.5-3.4 V (vs. Na/Na^+)
Reversible Capacity	≈140 mAh g^{-1}	≈120 mAh g^{-1}

Table 1 shows the main characteristics of both $LiCoO_2$ and P2-Na_xCoO_2. Although both P2-Na_xCoO_2 and $LiCoO_2$ can be assigned to the same crystal system consisting of edge-sharing CoO_6 octahedra sheets, due to the different properties of Na^+ and Li^+ ions, the two cathodes show

ACCEPTED MANUSCRIPT

various electrochemical characteristics.[161] To begin with, due to the larger ionic radius of Na^+, the P2-Na_xCoO_2 has a lower ion diffusion rate than $LiCoO_2$. Then, as can be seen in Fig. 20,[161] after charged to >100 mAh g^{-1}, the difference in voltage of the two materials is approximately 0.4 V. It is believed that this difference is caused by the difference in various standard electrochemical potentials for Li (3.04 V) and Na (2.71 V). Besides, the reversible capacity of P2-Na_xCoO_2 is lower than $LiCoO_2$. As a result, the available energy density is much lower in the sodium ion battery based on P2-Na_xCoO_2 cathode when the same chemistry (redox species and host crystal structures) with the lithium ion battery based on $LiCoO_2$ cathode.

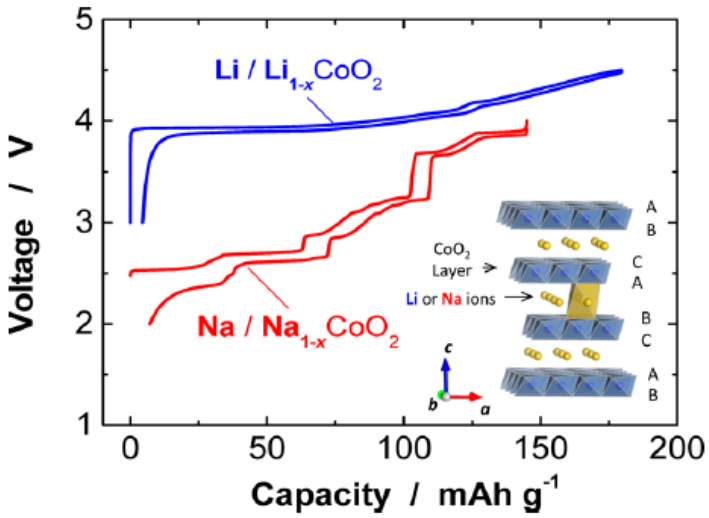


Fig. 20 Comparison of charge/discharge curves of Li/$LiCoO_2$ and Na/$NaCoO_2$ cells.[161]

To understand the electrochemical behaviour of P2-Na_xCoO_2, the materials with different Na^+ compositions of were investigated systematically. Three main factors cause the cationic redistribution, including the electrostatic repulsion between Na^+ ion in different planes, the repulsion between Na^+ and Co^{3+} through the common face of different polyhedra and the electronic interaction in the Co layer. The schematic of cationic redistribution in P2-Na_xCoO_2 is described in Fig. 21. The experimental result shows that the distribution of cationic ions has a significant impact on the electronic properties. Even a slight deviation (about 1% or 2%) can form a new distribution of the Na^+ ions. Thus, the investigation of P2-Na_xCoO_2 materials and their electrochemical performances is varied and interesting.[157]

ACCEPTED MANUSCRIPT

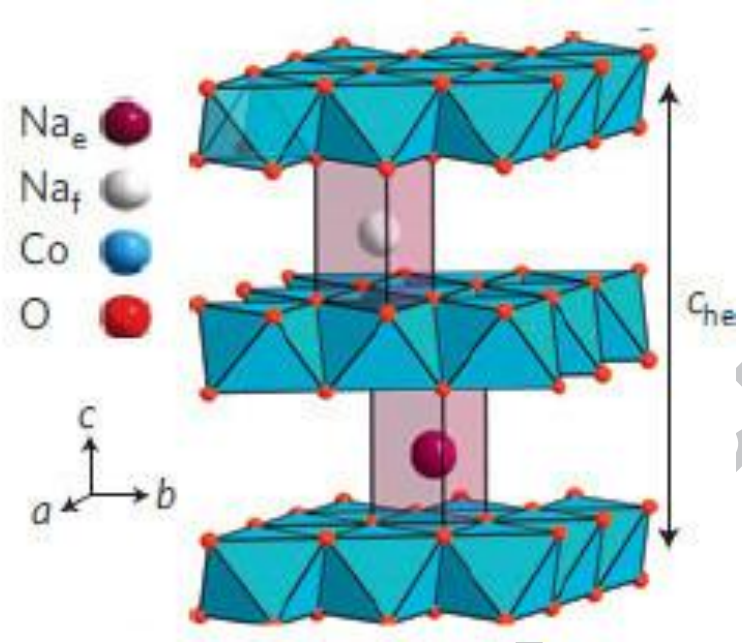


Fig. 21 Na^+/vacancy ordering in the interslab space of the lamellar structure of P2-Na_xCoO_2 phases.[157]

As cathode material for SIB, the main disadvantage of P2-Na_xCoO_2 is its poor cycling performance.[162] To solve this problem, several methods have been introduced such as morphology controlling, introduction of conductive substrate and cation doping. Recent work by Lou's group proved that regular morphology and microsize can prolong the cycling life and improve the volumetric energy density of $Na_{0.7}CoO_2$.[163] Such $Na_{0.7}CoO_2$ was synthesized by a facile strategy. As shown in Fig. 22, regular sized $CoCO_3$ was used as the precursor, with the final product, regular-$Na_{0.7}CoO_2$ (r-NCO), maintaining a spherical morphology with a size of about 5 μm. Between the operating voltage range of 2.0-3.8 V (*vs.* Na/Na^+), this material offers a high specific capacity of 125 mAh g^{-1} at 0.04 C (about 5 mA g^{-1}). After 300 cycles, at 0.4 C, 86% capacity is preserved for the regular $Na_{0.7}CoO_2$, which is remarkably higher than that of the irregular version (only a low capacity retention of 46% after 200 cycles can be observed for irregular $Na_{0.7}CoO_2$). Even at a large rate of 16 C (about 2 A g^{-1}), regular $Na_{0.7}CoO_2$, still demonstrates a high specific capacity of 64 mAh g^{-1}, presenting excellent rate capability.

ACCEPTED MANUSCRIPT

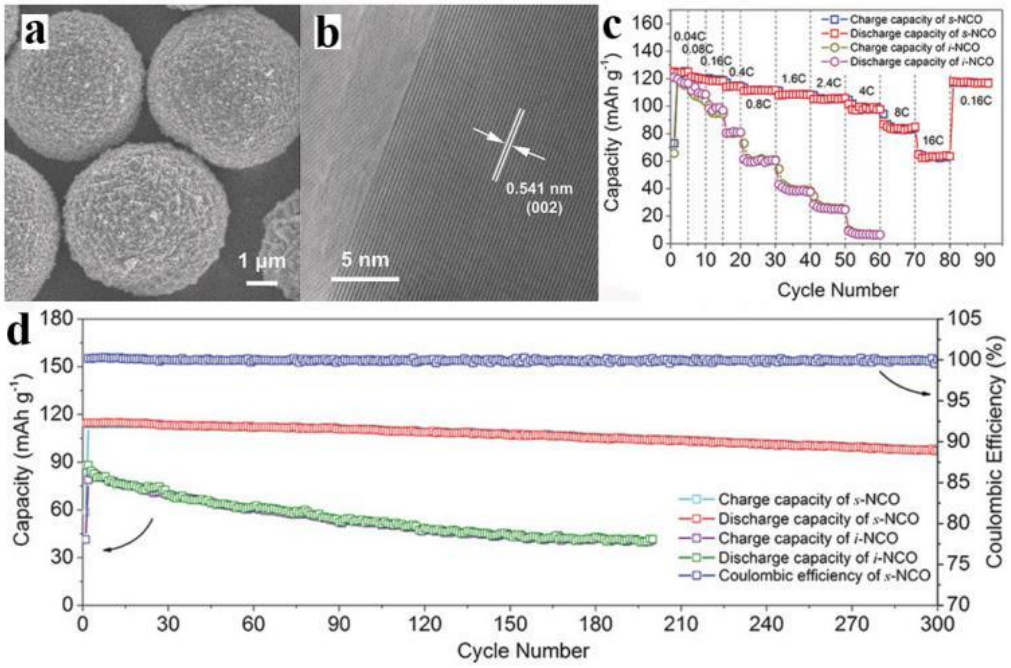


Fig. 22 (a) FESEM images and (b) HRTEM image of P2-$Na_{0.7}CoO_2$ microspheres. (c) Rate performance of s-NCO and irregular-NCO (i-NCO), and (d) Cycling performance of s-NCO and i-NCO at a current rate of 0.4 C and the corresponding Coulombic efficiency of s-NCO. (Note: 1C=125 mAh g^{-1}.)[163]

Nanocrystallization is another effective strategy to improve the electrochemical performance of electrode materials. Engineering $Na_{0.7}CoO_2$ arrays upon Ni foam can control the size and morphology of this sodium cobaltates.[164] As shown in Fig. 23, open architecture $Na_{0.7}CoO_2$ nanosheets can orderly grow on Ni foam. This composite shows a high areal capacity of 1.16 mAh cm^{-2} at 1 C, with a prolonged cycling life being obtained. More than 50 $mAhg^{-1}$ capacity can be preserved after 1100 cycles, at 6 C. Furthermore, at a larger rate of 15 C, a capacity of 57.8 $mAhg^{-1}$ maintains. However, although the Ni foam substrate can bring significant advantages, such as binder free, high conductivity, open ion diffusion pathway, it will also reduce the energy density because Ni does not offer capacity.

ACCEPTED MANUSCRIPT

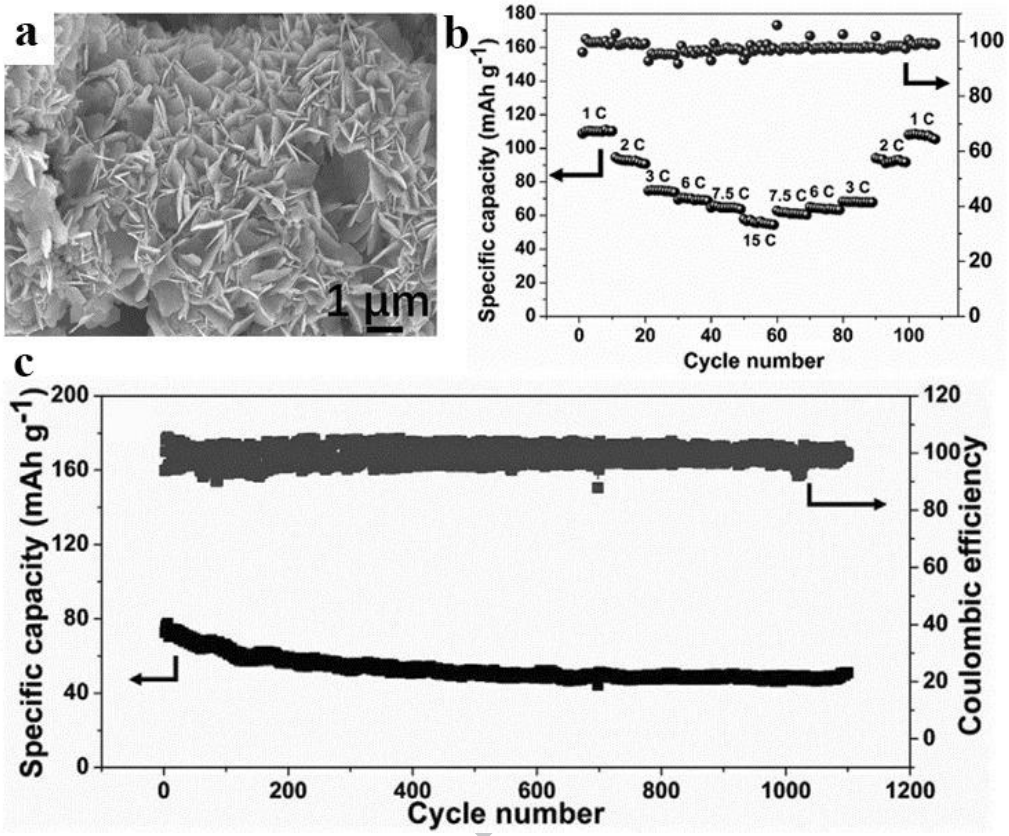


Fig. 23 (a) SEM images of $Na_{0.7}CoO_2$ arrays. (b) Rate performance at various current rates and Cycling performance of the $Na_{0.7}CoO_2$ electrode at a current rate of 6 C.[164]

It is believed that the cationic substitution improves the cycling life due to the suppression of the Na^+/vacancy ordering condition.[165-167] Theoretical calculation results suggest that the P2-$Na_xNi_yCo_{1-y}O_2$ cathodes ($x=0.66$ or 0.75, and $0\leq y\leq 0.33$) are thermodynamically stable or metastable.[168] Therefore, a new type of P2-type layered transition metal oxide, $Na_{0.75}Ni_{0.22}Co_{0.78}O_2$, has been synthesized by Bianchini and co-workers. The introduction of nickel can increase the capacity and raise the average discharge voltage to ~3V. However, the cycling performance and Coulombic efficiency of this material should be further optimized. Further investigations by Kang et al. have considered the effect of titanium substitution upon the P2-Na_xCoO_2.[169] However, the content of Ti should not be higher than 10%, otherwise an unfavorable crystal phase is formed. Compared with pristine, the $Na_{0.67}CoO_2$, $Na_{0.67}Co_{0.90}Ti_{0.10}O_2$ possesses an improved cycling life and larger energy density. It should be noted that if the content of Ti increases more than 10%, the rate capability will decrease.

Over recent years, P2-Na_xCoO_2 has been regarded as an available cathode material for solid

ACCEPTED MANUSCRIPT

state SIBs. For example, a novel solid state sodium polymer battery consisting of a $Na_{0.7}CoO_2$ cathode, PEO-based electrolyte and Na metal anode has been reported by Singh et al.[170] Under the optimized conditions, this battery exhibits a specific capacity of ~138 mAh g^{-1} at 0.1 C with a Coulombic efficiency of 99%. To further enhance the electrochemical performance, $Na_{0.7}CoO_2$ material that can be combined with some sodium oxyacids.[153] Briefly, $Na_{0.7}CoO_2$ when ball-milled with several sodium oxyacids (including $NaNO_3$, Na_2SO_4, Na_3PO_4, $NaBO_3$ or Na_2CO_3), can form an amorphous cathode material. It should be pointed that when tested in a cell with a Na_3PS_4 solid electrolyte, the sodium oxyacids can enhance the malleability and ionic conductivity of $Na_{0.7}CoO_2$. In particular, $Na_{0.7}CoO_2$-$NaNO_3$ hybrid cathodes shows the highest ionic conductivity and capacity of 170 mAh g^{-1} in the 5th cycle. However, the rate capability of solid sodium battery assembled by P2-$Na_{0.7}CoO_2$ cathode should be further improved.

Table 2 exhibits a summary of the synthesis methods and Na^+ ion storage properties of some above-mentioned materials.

ACCEPTED MANUSCRIPT

ACCEPTED MANUSCRIPT

Table 2. Systhesis methods and Na^+ ion storage performances of various cobaltiferous electrodes

Material description	**Synthesis method**	**Current density**	**Capacity**	**Cycle number**	**Ref.**
Co_3O_4@nitrogen-doped carbon	ZIF-67 as precursor, calcination in Ar and air atmospheres, respectively	1000 mA g^{-1}	175 mAh g^{-1}	1100 cycles	[80]
Co_3O_4-graphene composite	$(C_2H_3O_2)_2Co$-$4H_2O$ as cobalt source, hydrothermal synthesis	100 mA g^{-1}	541 mAh g^{-1}	50 cycles	[81]
Co_3O_4 sheets/3D graphene networks	$Co(NO_3)_2$-$6H_2O$ as cobalt source, hexamethylenetetramine as carbon source, hydrothermal synthesis and annealing in air	25 mA g^{-1}	534 mAh g^{-1}	50 cycles	[87]
GO/SnO_2/Co_3O_4	$Co(NO_3)_2$-$6H_2O$ as cobalt source, hydrothermal synthesis	1000 mA g^{-1}	241 mAh g^{-1}	500 cycles	[90]
CoO microsphere	$CoSO_4$-$7H_2O$ as cobalt source, Cu foil as substrate, hydrothermal synthesis and annealing in Ar	100 mA g^{-1}	499 mAh g^{-1}	250 cycles	[94]
Co_9S_8-quantum dots@ 3D ordered microporous N-doped carbon framework	$CoCl_2 \cdot 6H_2O$ and sodium oleate mixed to form cobalt-oleate complex precursor, thiourea as carbon source and sulfur source, SiO_2 nanospheres as template, calcination in Ar	1000 mA g^{-1}	345 mAh g^{-1}	2000 cycles	[99]
yolk-shelled Co_9S_8/MoS_2.carbon	ZIF-67 as precursor, sulfur powder as sulfur source, heating in H_2/Ar atmosphere	2000 mA g^{-1}	421 mAh g^{-1}	250 cycles	[103]
CoS_2 hollow microstructures	$CoSO_4$-$7H_2O$ as cobalt source, $Na_2S_2O_3$-$5H_2O$ as sulfur source, Hydrothermal synthesis	100 mA g^{-1}	240 mAh g^{-1}	800 cycles	[104]

ACCEPTED MANUSCRIPT

Table 2 (Contd.)

Material description	Synthesis method	Current density	Capacity	Cycle number	Ref.
N-doped polygonal CoS_2@C	$Co(CH_3COO)_2$-$4H_2O$ as cobalt source, thiourea as sulfur source, glucose as carbon source, CTAB as nitrogen source, solvothermal synthesis in ethylene glycol	1000 mA g^{-1}	559 mAh g^{-1}	1000 cycles	[107]
double-morphology CoS_2@N-doped carbon nanofibers	$Co(CH_3COO)_2$-$4H_2O$ as cobalt source, Thiourea and sulfur powder as sulfur source, solvothermal synthesis in ethylene glycol and heating in Ar atmosphere	1000 mA g^{-1}	620 mAh g^{-1}	900 cycles	[113]
CoS nanoparticles/N-doped carbon nanorods	Co-MOF as precursor, sublimed sulfur powder as sulfur source, calcination under vacuum atmosphere	1000 mA g^{-1}	542 mAh g^{-1}	2000 cycles	[119]
CoS@alveolus-like carbon yolk-shell microsphere	$Co(NO_3)_2 \cdot 6H_2O$ as cobalt source, thioacetamide as sulfur source, SiO_2 nanospheres as template, polymeric layer coating, calcination under vacuum atmosphere	200 mA g^{-1}	532 mAh g^{-1}	100 cycles	[129]
urchin-like $CoSe_2$	$CoSO_4$-$7H_2O$ as cobalt source, Se powder as selenium source, solvothermal synthesis in DMF	1000 mA g^{-1}	410 mAh g^{-1}	1800 cycles	[132]
hollow polyhedrons structured $CoSe_2$@C bridged by CNTs	ZIF-67 as precursor, annealing in H_2/Ar atmosphere to form Co@C/CNTs, then heated with Se powder in in H_2/Ar atmosphere one more time	1000 mA g^{-1}	390 mAh g^{-1}	1000 cycles	[136]
$Co_{0.85}Se$@reduced graphene oxide	$Co(NO_3)_2 \cdot 5H_2O$ as cobalt source, Se powder as selenium source, solvothermal synthesis	1000 mA g^{-1}	382 mAh g^{-1}	800 cycles	[140]

ACCEPTED MANUSCRIPT

Table 2 (Contd.)

Material description	Synthesis method	Current density	Capacity	Cycle number	Ref.
$Co_{0.85}Se$ nanosheets/graphene	$Co(CH_3COO)_2$-$4H_2O$ as cobalt source, Na_2SeO_3 as selenium source, solvothermal synthesis in a diethylenetriamine/water mixture	2000 mA g^{-1}	112 mAh g^{-1}	500 cycles	[141]
CoSe@carbon spheres	$Co(NO_3)_2 \cdot 6H_2O$ as cobalt source, H_3O_2Se as selenium source, glycerol as carbon source, solvothermal synthesis in isopropanol and annealing in N_2	4000 mA g^{-1}	260 mAh g^{-1}	10000 cycles	[145]
CoP@polypyrrole nanowires/carbon paper	$Co(NO_3)_2$-$6H_2O$ as cobalt source, NaH_2PO_2-H_2O as phosphorus source, carbon fiber as substrate, hydrothermal synthesis and annealing in Ar	1.5 mA cm^{-2}	0.443 mAh cm^{-2}	1000 cycles	[151]
CoP@C-reduced graphene oxide-nickel foam composite	ZIF-67 as precursor, NaH_2PO_2-H_2O as phosphorus source, Phosphidation in Ar	100 mA g^{-1}	473.1 mAh g^{-1}	100 cycles	[152]
P2-$Na_{0.7}CoO_2$ Microspheres	$CoCl_2$-$6H_2O$ as cobalt source, Na_2CO_3 as sodium source, solvothermal synthesis and heating in air atmosphere	0.4 C	About 98 mAh g^{-1}	300 cycles	[163]
$Na_{0.7}CoO_2$ nanosheet arrays on Ni foam	$Co(NO_3)_2$-$6H_2O$ as cobalt source, NaOH as sodium source, Ni foams as substrate, hydrothermal synthesis and calcination in air	6 C	51 mAh g^{-}	1100 cycles	[164]

ACCEPTED MANUSCRIPT

7. Conclusion and Outlook

As a promising candidate for grid-scale energy storage, SIBs have attracted great attention due to the low-cost of sodium resources and electrochemical characteristics similar to those of LIBs. From the commercialization perspective, the primary parameters are the production and operation costs and long-term cycling capability. During the past few years, some achievements have already built upon the electrode material for SIB with high energy density and long cycle stability comparable to LIB counterparts. In addition, some new understanding of the Na^+ ion intercalation chemistry offers new design ideas for novel electrode materials that are potentially low-cost and scalable for manufacture. As a result, some classic materials with a long research history have been revitalized, including cobalt-based materials. Cobalt-based materials, as cathode or anode materials, are promising candidates for achieving high-performance SIBs for large-scale energy storage applications. The structure and specific capacities (practical and theoretical values) of representative cobalt-based materials reported in recent years for SIBs are a foundation of SIB development based on LIBs and the knowledge from conversion mode systems and Li-S systems.

The layered P2-Na_xCoO_2, which has a longer history than $LiCoO_2$, faces the challenge of sufficient cycling stability because of the unavoidable intrinsic complex structural redistribution during Na^+ insertion/extraction. Using a strategy of suitable element doping/substitution, the fast degradation in the capacity may be mitigated or suppressed. This is a promising way to overcome the inherent defects of P2-Na_xCoO_2. Combined with rational structure design, the future of this layered metal oxide and its isostructural counterparts are expected to be useful in SIB electrode development.

For anode materials, various cobalt oxides, sulfides and selenides are all hindered by the conversion reactions, which creates shortcomings such as low reversibility, sluggish kinetics and large volume change especially when deep discharged to lower voltages. Although conversion reactions can deliver high theoretical capacities, most of the electrodes exhibit reversible capacities (in a limited voltage window) far lower than the theoretical values, indicating that oxide-based anodes require alternative material developments to offset low voltage influence on energy density for SIBs, as is te case for LIBs. One approach that tackles NA^+ insertion and volumetric expansion is carbon coating and electrical wiring. Another is the development of binder and conductive additive-free formulations that offset energy density loss to some degree, in

ACCEPTED MANUSCRIPT

cases where the lower voltage range is limited to avoid conversion reactions. This approach saves weight in the electrode formation. Cobalt chalcogenides have the higher conductivities than their metal oxide counterparts do. Thus, they are more promising than cobalt oxides for SIBs. It should be noted that the final products of the conversion reaction, Na_2S and Na_2Se, are similar to the Na-S battery and Na-Se battery. Maybe a successful strategy in these two fields are also effective to enhance the electrochemical performance of cobalt chalcogenides. In addition, the relationship between an ether-based electrolyte and the electrochemical behaviors of the cobalt-based anode should be studied more systematically in future.

By increasing the detail of the electrode design, such as with carbon decoration and nanostructuring, the cycle stability and rate capability can still be improved. Although many significant challenges lie ahead, the rapid advances in recent years by many researchers, together with the sustained interest from industrial and academic communities, indicate that cobalt-based electrode materials are worth further investigation in the pursuit of low-cost, long-term life of SIBs.

Acknowledgements

This work was supported by the National Natural Science Foundation of China (Grant No. 51302079), and the Natural Science Foundation of Hunan Province (Grant No. 2017JJ1008).

References

[1] Z. Su, Z. Wei, C. Lai, H. Deng, Z. Liu, J. Ma, Robust pseudo-capacitive Li-I_2 battery enabled by catalytic, adsorptive N-doped graphene interlayer, Energy Storage Materials 14 (2018) 129-135.

[2] L. Wang, Y. Wang, M. Wu, Z. Wei, C. Cui, M. Mao, J. Zhang, X. Han, Q. Liu, J. Ma, Nitrogen, fluorine, and boron ternary doped carbon fibers as cathode electrocatalysts for zinc-air batteries, Small 14 (2018) 1800737.

[3] M. Wu, Y. Wang, Z. Wei, L. Wang, M. Zhuo, J. Zhang, X. Han, J. Ma, Ternary doped porous carbon nanofibers with excellent ORR and OER performance for zinc–air batteries, Journal of Materials Chemistry A 6 (2018) 10918-10925.

[4] Y. Fang, Z. Chen, L. Xiao, X. Ai, Y. Cao, H. Yang, Recent progress in iron-based electrode materials for grid-scale sodium-ion batteries, Small 14 (2018) 1703116.

ACCEPTED MANUSCRIPT

[5] H. Pan, Y.-S. Hu, L. Chen, Room-temperature stationary sodium-ion batteries for large-scale electric energy storage, Energy & Environmental Science 6 (2013) 2338-2360.
[6] Y. Sun, N. Liu, Y. Cui, Promises and challenges of nanomaterials for lithium-based rechargeable batteries, Nature Energy 1 (2016) 16071.
[7] D. Bruce, K. Haresh, T. Jean-Marie, Electrical energy storage for the grid: a battery of choices, Science 334 (2011) 928-935.
[8] V. Aravindan, Y.-S. Lee, S. Madhavi, Research progress on negative electrodes for practical Li-ion batteries: Beyond carbonaceous anodes, Advanced Energy Materials 5 (2015) 1402225.
[9] J. Liu, J. Liang, C. Wang, J. Ma, Electrospun CoSe@N-doped carbon nanofibers with highly capacitive Li storage, Journal of Energy Chemistry 33 (2019) 160-166.
[10] J. Liang, Z. Wei, C. Wang, J. Ma, Vacancy-induced sodium-ion storage in N-doped carbon Nanofiber@MoS_2 nanosheet arrays, Electrochimica Acta 285 (2018) 301-308.
[11] M.D. Slater, D. Kim, E. Lee, C.S. Johnson, Sodium-ion batteries, Advanced Functional Materials 23 (2013) 947-958.
[12] J. Huang, Z. Wei, J. Liao, W. Ni, C. Wang, J. Ma, Molybdenum and tungsten chalcogenides for lithium/sodium-ion batteries: Beyond MoS_2, Journal of Energy Chemistry 33 (2019) 100-124.
[13] Z. Wei, L. Wang, M. Zhuo, W. Ni, H. Wang, J. Ma, Layered tin sulfide and selenide anode materials for Li- and Na-ion batteries, Journal of Materials Chemistry A 6 (2018) 12185-12214.
[14] Q. Wang, J. Xu, W. Zhang, M. Mao, Z. Wei, L. Wang, C. Cui, Y. Zhu, J. Ma, Research progress on vanadium-based cathode materials for sodium ion batteries, Journal of Materials Chemistry A 6 (2018) 8815-8838.
[15] N. Ortiz-Vitoriano, N.E. Drewett, E. Gonzalo, T. Rojo, High performance manganese-based layered oxide cathodes: overcoming the challenges of sodium ion batteries, Energy & Environmental Science 10 (2017) 1051-1074.
[16] V. Palomares, P. Serras, I. Villaluenga, K.B. Hueso, J. Carretero-González, T. Rojo, Na-ion batteries, recent advances and present challenges to become low cost energy storage systems, Energy & Environmental Science 5 (2012) 5884-5901.
[17] C. Fang, Y. Huang, W. Zhang, J. Han, Z. Deng, Y. Cao, H. Yang, Routes to high energy cathodes of sodium-ion batteries, Advanced Energy Materials 6 (2016) 1501727.
[18] M.H. Han, E. Gonzalo, G. Singh, T. Rojo, A comprehensive review of sodium layered oxides: powerful cathodes for Na-ion batteries, Energy & Environmental Science 8 (2015) 81-102.
[19] W. Chen, X. Zhang, L. Mi, C. Liu, J. Zhang, S. Cui, X. Feng, Y. Cao, C. Shen, High-performance flexible freestanding anode with hierarchical 3D carbon-networks/Fe_7S_8/graphene for applicable sodium-ion batteries, Adv Mater 31 (2019) 1806664.
[20] S. Qi, L. Mi, K. Song, K. Yang, J. Ma, X. Feng, J. Zhang, W. Chen, Understanding shuttling effect in sodium ion batteries for the solution of capacity fading: FeS_2 as an example, The Journal of Physical Chemistry C 123 (2019) 2775-2782.
[21] H. Hou, X. Qiu, W. Wei, Y. Zhang, X. Ji, Carbon anode materials for advanced sodium-ion batteries, Advanced Energy Materials 7 (2017) 1602898.
[22] Y. Wen, K. He, Y. Zhu, F. Han, Y. Xu, I. Matsuda, Y. Ishii, J. Cumings, C. Wang, Expanded graphite as superior anode for sodium-ion batteries, Nat Commun 5 (2014) 4033.

ACCEPTED MANUSCRIPT

[23] W. Chen, S. Qi, L. Guan, C. Liu, S. Cui, C. Shen, L. Mi, Pyrite FeS_2 microspheres anchoring on reduced graphene oxide aerogel as an enhanced electrode material for sodium-ion batteries, Journal of Materials Chemistry A 5 (2017) 5332-5341.
[24] Y. Zhao, L.P. Wang, M.T. Sougrati, Z. Feng, Y. Leconte, A. Fisher, M. Srinivasan, Z. Xu, A Review on design strategies for carbon based metal oxides and sulfides nanocomposites for high performance Li and Na ion battery anodes, Advanced Energy Materials 7 (2017) 1601424.
[25] J. Cui, S. Yao, J.-K. Kim, Recent progress in rational design of anode materials for high-performance Na-ion batteries, Energy Storage Materials 7 (2017) 64-114.
[26] L. Wang, Z. Wei, M. Mao, H. Wang, Y. Li, J. Ma, Metal oxide/graphene composite anode materials for sodium-ion batteries, Energy Storage Materials 16 (2019) 434-454.
[27] C. Cui, Z. Wei, J. Xu, Y. Zhang, S. Liu, H. Liu, M. Mao, S. Wang, J. Ma, S. Dou, Three-dimensional carbon frameworks enabling MoS_2 as anode for dual ion batteries with superior sodium storage properties, Energy Storage Materials 15 (2018) 22-30.
[28] A. Bhide, J. Hofmann, A.K. Durr, J. Janek, P. Adelhelm, Electrochemical stability of non-aqueous electrolytes for sodium-ion batteries and their compatibility with $Na_{0.7}CoO_2$, Phys Chem Chem Phys 16 (2014) 1987-1998.
[29] S. Hwang, Y. Lee, E. Jo, K.Y. Chung, W. Choi, S.M. Kim, W. Chang, Investigation of thermal stability of P2-Na_xCoO_2 cathode materials for sodium ion batteries using real-time electron microscopy, ACS Appl Mater Interfaces 9 (2017) 18883-18888.
[30] P. Vassilaras, X. Ma, X. Li, G. Ceder, Electrochemical properties of monoclinic $NaNiO_2$, Journal of The Electrochemical Society 160 (2012) A207-A211.
[31] J. Zhao, L. Zhao, K. Chihara, S. Okada, J.I. Yamaki, S. Matsumoto, S. Kuze, K. Nakane, Electrochemical and thermal properties of α-$NaFeO_2$ cathode for Na-ion batteries, Journal of Power Sources 244 (2013) 752-757.
[32] J.-J. Ding, Y.-N. Zhou, Q. Sun, Z.-W. Fu, Cycle performance improvement of $NaCrO_2$ cathode by carbon coating for sodium ion batteries, Electrochemistry Communications 22 (2012) 85-88.
[33] Y. Zhu, Y. Xu, Y. Liu, C. Luo, C. Wang, Comparison of electrochemical performances of olivine NaFePO4 in sodium-ion batteries and olivine $LiFePO_4$ in lithium-ion batteries, Nanoscale 5 (2013) 780-787.
[34] X. Rui, W. Sun, C. Wu, Y. Yu, Q. Yan, An advanced sodium-ion battery composed of carbon coated $Na_3V_2(PO_4)_3$ in a porous graphene network, Adv Mater 27 (2015) 6670-6676.
[35] R.A. Shakoor, D.-H. Seo, H. Kim, Y.-U. Park, J. Kim, S.-W. Kim, H. Gwon, S. Lee, K. Kang, A combined first principles and experimental study on $Na_3V_2(PO4)_2F_3$ for rechargeable Na batteries, Journal of Materials Chemistry 22 (2012) 20535-20541.
[36] F. Sauvage, E. Quarez, J.M. Tarascon, E. Baudrin, Crystal structure and electrochemical properties vs. Na^+ of the sodium fluorophosphate $Na_{1.5}VOPO_4F_{0.5}$, Solid State Sciences 8 (2006) 1215-1221.
[37] R. Tripathi, S.M. Wood, M.S. Islam, L.F. Nazar, Na-ion mobility in layered Na_2FePO_4F and olivine $Na[Fe,Mn]PO_4$, Energy & Environmental Science 6 (2013) 2257-2264.
[38] C. Li, C. Yin, X. Mu, J. Maier, Top-down synthesis of open framework fluoride for lithium and Sodium Batteries, Chemistry of Materials 25 (2013) 962-969.

ACCEPTED MANUSCRIPT

[39] C.P. Guntlin, T. Zünd, K.V. Kravchyk, M. Wörle, M.I. Bodnarchuk, M.V. Kovalenko, Nanocrystalline FeF_3 and MF_2 (M = Fe, Co, and Mn) from metal trifluoroacetates and their Li(Na)-ion storage properties, Journal of Materials Chemistry A 5 (2017) 7383-7393.
[40] Q. Zhao, Y. Lu, J. Chen, Advanced organic electrode materials for rechargeable sodium-ion batteries, Advanced Energy Materials 7 (2017) 1601792.
[41] X. Li, J. Ni, S.V. Savilov, L. Li, Materials based on antimony and bismuth for sodium storage, Chemistry-A European Journal 24 (2018) 13719-13727.
[42] L.P. Wang, L. Yu, X. Wang, M. Srinivasan, Z.J. Xu, Recent developments in electrode materials for sodium-ion batteries, Journal of Materials Chemistry A 3 (2015) 9353-9378.
[43] Z. Hu, Q. Liu, S.L. Chou, S.X. Dou, Advances and challenges in metal sulfides/selenides for next-generation rechargeable sodium-ion batteries, Adv Mater 29 (2017) 1700606 .
[44] Y. Xiao, S.H. Lee, Y.-K. Sun, The application of metal sulfides in sodium ion batteries, Advanced Energy Materials 7 (2017) 1601329.
[45] Y. Liang, Y. Li, H. Wang, J. Zhou, J. Wang, T. Regier, H. Dai, Co_3O_4 nanocrystals on graphene as a synergistic catalyst for oxygen reduction reaction, Nat Mater 10 (2011) 780-786.
[46] W. Koshibae, K. Tsutsui, S. Maekawa, Thermopower in cobalt oxides, Phys.rev.b 62 (2000) 6869-6872.
[47] X.W. Hu, S. Liu, B.T. Qu, X.Z. You, Starfish-shaped $Co_3O_4/ZnFe_2O_4$ hollow nanocomposite: synthesis, supercapacity, and magnetic properties, ACS Appl Mater Interfaces 7 (2015) 9972-9981.
[48] N. Du, H. Zhang, B.D. Chen, J.B. Wu, X.Y. Ma, Z.H. Liu, Y.Q. Zhang, D.R. Yang, X.H. Huang, J.P. Tu, Porous Co_3O_4 nanotubes derived from $Co_4(CO)_{12}$ clusters on carbon nanotube templates: A highly efficient material for Li-battery applications, Advanced Materials 19 (2007) 4505-4509.
[49] X.W. Lou, D. Deng, J.Y. Lee, J. Feng, L.A. Archer, Self-supported formation of needlelike Co_3O_4 nanotubes and their application as lithium-ion battery electrodes, Advanced Materials 20 (2008) 258-262.
[50] Z. Jian, P. Liu, F. Li, M. Chen, H. Zhou, Monodispersed hierarchical Co_3O_4 spheres intertwined with carbon nanotubes for use as anode materials in sodium-ion batteries, Journal of Materials Chemistry A 2 (2014) 13805-13809.
[51] S. Dong, S. Wang, J. Guan, S. Li, Z. Lan, C. Chen, C. Shang, L. Zhang, X. Wang, L. Gu, G. Cui, L. Chen, Insight into enhanced cycling performance of Li-O_2 batteries based on binary $CoSe_2$/CoO nanocomposite electrodes, J Phys Chem Lett 5 (2014) 615-621.
[52] W.H. Wang, J.L. Zhang, B.H. Li, L. Shi, Electrochemical investigation of Sn-Co alloys as anode for Na-ion batteries, Journal of Alloys and Compounds 780 (2019) 565-569.
[53] H. Matsumoto, H. Sakaebe, K. Tatsumi, M. Kikuta, E. Ishiko, M. Kono, Fast cycling of Li/$LiCoO_2$ cell with low-viscosity ionic liquids based on bis(fluorosulfonyl)imide[$FSI]^-$, Journal of Power Sources 160 (2006) 1308-1313.
[54] X. Xia, J.R. Dahn, A study of the teactivity of de-intercalated P2-Na_xCoO_2 with non-Aqueous solvent and electrolyte by accelerating rate calorimetry, Journal of the Electrochemical Society 159 (2012) A647-A650.
[55] J.-W. Wen, D.-W. Zhang, Y. Zang, X. Sun, B. Cheng, C.-X. Ding, Y. Yu, C.-H. Chen, Li and Na storage behavior of bowl-like hollow Co_3O_4 microspheres as an anode material for lithium-ion and sodium-ion batteries, Electrochimica Acta 132 (2014) 193-199.

ACCEPTED MANUSCRIPT

[56] W. Kang, Y. Zhang, L. Fan, L. Zhang, F. Dai, R. Wang, D. Sun, Metal-organic framework derived porous hollow Co_3O_4/N-C polyhedron composite with excellent energy storage capability, ACS Appl Mater Interfaces 9 (2017) 10602-10609.
[57] G.D. Park, Y.C. Kang, One-pot synthesis of $CoSe_x$-rGO composite powders by spray pyrolysis and their application as anode material for sodium-ion batteries, Chemistry 22 (2016) 4140-4146.
[58] S.-K. Park, J.K. Kim, Y. Chan Kang, Metal–organic framework-derived $CoSe_2$/(NiCo)Se_2 box-in-box hollow nanocubes with enhanced electrochemical properties for sodium-ion storage and hydrogen evolution, Journal of Materials Chemistry A 5 (2017) 18823-18830.
[59] F. Han, C. Zhang, B. Sun, W. Tang, J. Yang, X. Li, Dual-carbon phase-protective cobalt sulfide nanoparticles with cable-type and mesoporous nanostructure for enhanced cycling stability in sodium and lithium ion batteries, Carbon 118 (2017) 731-742.
[60] J.R. Wilson, J.S. Cronin, S.A. Barnett, S.J. Harris, Measurement of three-dimensional microstructure in a $LiCoO_2$ positive electrode, Journal of Power Sources 196 (2016) 3443-3447.
[61] T. Shibata, Y. Fukuzumi, W. Kobayashi, Y. Moritomo, Fast discharge process of layered cobalt oxides due to high Na^+ diffusion, Sci. Rep. 5 (2015) 9006.
[62] H. Yu, Z.L. Brown, C. Wei, M.N. Obrovac, Thermoelectrochemical activation of CoO in Na cells, Journal of the Electrochemical Society 165 (2018) A1595-A1600.
[63] Z. Mao, M. Zhou, K. Wang, W. Wang, H. Tao, K. Jiang, Electrospinning synthesis of Co_3O_4@C nanofibers as a high-performance anode for sodium ion batteries, RSC Advances 7 (2017) 23122-23126.
[64] B. Fu, X. Zhou, Y. Wang, Co_3O_4 carbon nanofiber mats as negative electrodes for sodium-ion batteries, Materials Letters 170 (2016) 21-24.
[65] Y. Zhang, N. Wang, P. Xue, Y. Liu, B. Tang, Z. Bai, S. Dou, Co_9S_8@carbon nanospheres as high-performance anodes for sodium ion battery, Chemical Engineering Journal 343 (2018) 512-519.
[66] Y. Zhao, Q. Pang, Y. Meng, Y. Gao, C. Wang, B. Liu, Y. Wei, F. Du, G. Chen, Self-assembled CoS nanoflowers wrapped in reduced graphene oxides as the high-performance anode materials for sodium-ion batteries, Chem. Eur. J. 23 (2017) 13150-13157.
[67] H. Jia, M. Dirican, C. Chen, P. Zhu, C. Yan, X. Dong, Z. Du, J. Guo, J. Wang, F. Tang, J. Tao, X. Zhang, Carbon-coated CoS@rGO anode material with enhanced cyclic stability for sodium storage, Materials Letters 233 (2018) 158-161.
[68] C. Cui, Z. Wei, G. Zhou, W. Wei, J. Ma, L. Chen, C. Li, Quasi-reversible conversion reaction of $CoSe_2$/nitrogen-doped carbon nanofibers towards long-lifetime anode materials for sodium-ion batteries, Journal of Materials Chemistry A 6 (2018) 7088-7098.
[69] N. Zhang, X. Han, Y. Liu, X. Hu, Q. Zhao, J. Chen, 3D porous γ-Fe_2O_3@C nanocomposite as high-performance anode material of Na-ion batteries, Advanced Energy Materials 5 (2015) 1401123.
[70] D. Chen, L. Peng, Y. Yuan, Y. Zhu, Z. Fang, C. Yan, G. Chen, R. Shahbazian-Yassar, J. Lu, K. Amine, G. Yu, Two-dimensional holey Co_3O_4 nanosheets for high-rate alkali-ion batteries: From rational synthesis to in Ssitu probing, Nano Lett 17 (2017) 3907-3913.
[71] M.B. Sreedhara, A.L. Santhosha, A.J. Bhattacharyya, C.N.R. Rao, Composite of few-layer MoO_3 nanosheets with graphene as a high performance anode for sodium-ion batteries, Journal of Materials Chemistry A 4 (2016) 9466-9471.

ACCEPTED MANUSCRIPT

[72] M. Zhou, Y. Xu, C. Wang, Q. Li, J. Xiang, L. Liang, M. Wu, H. Zhao, Y. Lei, Amorphous TiO_2 inverse opal anode for high-rate sodium ion batteries, Nano Energy 31 (2017) 514-524.
[73] D. Xin, J. Dai, J. Liu, Q. Wang, W. Li, Mesocrystal hexagonal Co_3O_4 nanosheets for high performance lithium and sodium-ion batteries, Materials Letters 209 (2017) 388-391.
[74] Y. Dou, Y. Wang, D. Tian, J. Xu, Z. Zhang, Q. Liu, B. Ruan, J. Ma, Z. Sun, S.X. Dou, Atomically thin Co_3O_4 nanosheet-coated stainless steel mesh with enhanced capacitive Na^+ storage for high-performance sodium-ion batteries, 2D Materials 4 (2016) 015022.
[75] K.C. Klavetter, S. Garcia, N. Dahal, J.L. Snider, J. Pedro de Souza, T.H. Cell, M.A. Cassara, A. Heller, S.M. Humphrey, C.B. Mullins, Li- and Na-reduction products of meso-Co_3O_4 form high-rate, stably cycling battery anode materials, J. Mater. Chem. A 2 (2014) 14209-14221.
[76] Z. Jian, P. Liu, F. Li, M. Chen, H. Zhou, Monodispersed hierarchical Co_3O_4 spheres intertwined with carbon nanotubes for use as anode materials in sodium-ion batteries, Journal of Materials Chemistry A 2 (2014) 13805-13809.
[77] Q. Deng, L. Wang, J. Li, Electrochemical characterization of Co_3O_4/MCNTs composite anode materials for sodium-ion batteries, Journal of Materials Science 50 (2015) 4142-4148.
[78] Z. Wang, S. Zhang, L. Yue, B. Wu, J. Mi, Synthesis of Co_3O_4 nanocubes/CNTs composite with enhanced sodium storage performance, Solid State Ionics 312 (2017) 32-37.
[79] Y. Lu, E. Fong, Botanic chemistry enabled synthesis of 3D hollow metal oxides/carbon hybrids for ultra-high performance metal-ion batteries, Materials Today Energy 4 (2017) 89-96.
[80] Y. Wang, C. Wang, Y. Wang, H. Liu, Z. Huang, Superior sodium-ion storage performance of Co_3O_4@nitrogen-doped carbon: derived from a metal-organic framework, Journal of Materials Chemistry A 4 (2016) 5428-5435.
[81] H. Kim, H. Kim, H. Kim, J. Kim, G. Yoon, K. Lim, W.-S. Yoon, K. Kang, Understanding origin of voltage hysteresis in conversion reaction for Na rechargeable batteries: The case of cobalt oxides, Advanced Functional Materials 26 (2016) 5042-5050.
[82] G. Longoni, M. Fiore, J.-H. Kim, Y.H. Jung, D.K. Kim, C.M. Mari, R. Ruffo, Co_3O_4 negative electrode material for rechargeable sodium ion batteries: An investigation of conversion reaction mechanism and morphology-performances correlations, Journal of Power Sources 332 (2016) 42-50.
[83] H.-H. Li, Z.-Y. Li, X.-L. Wu, L.-L. Zhang, C.-Y. Fan, H.-F. Wang, X.-Y. Li, K. Wang, H.-Z. Sun, J.-P. Zhang, Shale-like Co_3O_4 for high performance lithium/sodium ion batteries, Journal of Materials Chemistry A 4 (2016) 8242-8248.
[84] Q. Li, J. Wu, J. Xu, V.P. Dravid, Synergistic sodiation of cobalt oxide nanoparticles and conductive carbon nanotubes (CNTs) for sodium-ion batteries, Journal of Materials Chemistry A 4 (2016) 8669-8675.
[85] M.M. Rahman, A.M. Glushenkov, T. Ramireddy, Y. Chen, Electrochemical investigation of sodium reactivity with nanostructured Co_3O_4 for sodium-ion batteries, Chem Commun 50 (2014) 5057-5060.
[86] M.M. Rahman, I. Sultana, Z. Chen, M. Srikanth, L.H. Li, X.J. Dai, Y. Chen, Ex situ electrochemical sodiation/desodiation observation of Co_3O_4 anchored carbon nanotubes: a high performance sodium-ion battery anode produced by pulsed plasma in a liquid, Nanoscale 7 (2015) 13088-13095.

ACCEPTED MANUSCRIPT

[87] Y. Liu, Z. Cheng, H. Sun, H. Arandiyan, J. Li, M. Ahmad, Mesoporous Co_3O_4 sheets/3D graphene networks nanohybrids for high-performance sodium-ion battery anode, Journal of Power Sources 273 (2015) 878-884.
[88] Y. Wu, J. Meng, Q. Li, C. Niu, X. Wang, W. Yang, W. Li, L. Mai, Interface-modulated fabrication of hierarchical yolk–shell Co_3O_4/C dodecahedrons as stable anodes for lithium and sodium storage, Nano Research 10 (2017) 2364-2376.
[89] H. Xu, G. Zhu, B. Hao, Metal-organic frameworks derived flower-like Co_3O_4/nitrogen doped graphite carbon hybrid for high-performance sodium-ion batteries, Journal of Materials Science & Technology 35 (2019) 100-108.
[90] X. Li, X. Sun, Z. Gao, X. Hu, R. Ling, S. Cai, C. Zheng, W. Hu, Highly reversible and fast sodium storage boosted by improved interfacial and surface charge transfer derived from the synergistic effect of heterostructures and pseudocapacitance in SnO_2-based anodes, Nanoscale 10 (2018) 2301-2309.
[91] G. Fang, J. Zhou, Y. Cai, S. Liu, X. Tan, A. Pan, S. Liang, Metal–organic framework-templated two-dimensional hybrid bimetallic metal oxides with enhanced lithium/sodium storage capability, Journal of Materials Chemistry A 5 (2017) 13983-13993.
[92] W. Zhang, Z. Yue, W. Miao, S. Liu, C. Fu, L. Li, Z. Zhang, H. Wang, Carbon-encapsulated tube-wire Co_3O_4/MnO_2 heterostructure nanofibers as anode material for sodium-ion batteries, Particle & Particle Systems Characterization 35 (2018) 1800138.
[93] Y. Han, J. Li, T. Zhang, P. Qi, S. Li, X. Gao, J. Zhou, X. Feng, B. Wang, Zinc/nickel-doped hollow core-shell Co_3O_4 derived from a metal-organic framework with high capacity, stability, and rate performance in lithium/sodium-ion batteries, Chemistry - A European Journal 24 (2017) 1651 -1656.
[94] L. Chang, K. Wang, L. Huang, Z. He, H. Shao, J. Wang, Hierarchically porous CoO microsphere films with enhanced lithium/sodium storage properties, Journal of Alloys and Compounds 725 (2017) 824-834.
[95] L. Chang, K. Wang, L.-a. Huang, Z. He, S. Zhu, M. Chen, H. Shao, J. Wang, Hierarchical CoO microflower film with excellent electrochemical lithium/sodium storage performance, J. Mater. Chem. A 5 (2017) 20892-20902.
[96] Y.V. Kaneti, J. Zhang, Y.-B. He, Z. Wang, S. Tanaka, M.S.A. Hossain, Z.-Z. Pan, B. Xiang, Q.-H. Yang, Y. Yamauchi, Fabrication of an MOF-derived heteroatom-doped Co/CoO/carbon hybrid with superior sodium storage performance for sodium-ion batteries, Journal of Materials Chemistry A 5 (2017) 15356-15366.
[97] H. Xia, K. Li, Y. Guo, J. Guo, Q. Xu, J. Zhang, CoS_2 nanodots trapped within graphitic structured N-doped carbon spheres with efficient performances for lithium storage, Journal of Materials Chemistry A 6 (2018) 7148-7154.
[98] X. Liu, H. Liu, Y. Zhao, Y. Dong, Q. Fan, Q. Kuang, Synthesis of the carbon-coated nanoparticle Co_9S_8 and its electrochemical performance as an anode material for sodium-ion batteries, Langmuir 32 (2016) 12593-12602.
[99] X. Hu, J. Jia, G. Wang, J. Chen, H. Zhan, Z. Wen, Reliable and general route to inverse opal structured nanohybrids of carbon-confined transition metal sulfides quantum dots for high-performance sodium storage, Advanced Energy Materials 8 (2018) 1801452.

ACCEPTED MANUSCRIPT

[100] Y. Zhao, Q. Pang, Y. Wei, L. Wei, Y. Ju, B. Zou, Y. Gao, G. Chen, Co_9S_8/Co as a high-performance anode for sodium-ion batteries with an ether-based electrolyte, ChemSusChem 10 (2017) 4778-4785.
[101] H. Wang, Y. Liang, Y. Li, H. Dai, $Co_{1-x}S$-graphene hybrid: a high-performance metal chalcogenide electrocatalyst for oxygen reduction, Angew Chem Int Ed Engl 50 (2011) 10969-10972.
[102] Z. Chen, R. Wu, M. Liu, H. Wang, H. Xu, Y. Guo, Y. Song, F. Fang, X. Yu, D. Sun, General synthesis of dual carbon-confined metal sulfides quantum dots toward high-performance anodes for sodium-ion batteries, Advanced Functional Materials 27 (2017) 1702046.
[103] Y. Wang, W. Kang, D. Cao, M. Zhang, Z. Kang, Z. Xiao, R. Wang, D. Sun, A yolk–shelled Co_9S_8/MoS_2-CN nanocomposite derived from a metal-organic framework as a high performance anode for sodium ion batteries, Journal of Materials Chemistry A 6 (2018) 4776-4782.
[104] X. Liu, K. Zhang, K. Lei, F. Li, Z. Tao, J. Chen, Facile synthesis and electrochemical sodium storage of CoS_2 micro/nano-structures, Nano Research 9 (2016) 198-206.
[105] Z. Li, W. Feng, Y. Lin, X. Liu, H. Fei, Flaky CoS_2 and graphene nanocomposite anode materials for sodium-ion batteries with improved performance, RSC Advances 6 (2016) 70632-70637.
[106] F. Han, T. Lv, B. Sun, W. Tang, C. Zhang, X. Li, In situ formation of ultrafine CoS_2 nanoparticles uniformly encapsulated in N/S-doped carbon polyhedron for advanced sodium-ion batteries, RSC Advances 7 (2017) 30699-30706.
[107] Y. Pan, X. Cheng, L. Gong, L. Shi, Y. Deng, H. Zhang, Highly reversible Na ion storage in N-doped polyhedral carbon-coated transition-metal chalcogenides by optimizing the nanostructure and surface engineering, Journal of Materials Chemistry A 6 (2018) 18967-18978.
[108] Y. Pan, X. Cheng, Y. Huang, L. Gong, H. Zhang, CoS_2 nanoparticles wrapping on flexible freestanding multichannel carbon nanofibers with high performance for Na-ion batteries, ACS Appl Mater Interfaces 9 (2017) 35820-35828.
[109] Z. Shadike, M.H. Cao, F. Ding, L. Sang, Z.W. Fu, Improved electrochemical performance of CoS_2-MWCNT nanocomposites for sodium-ion batteries, Chem Commun 51 (2015) 10486-10489.
[110] K. Xie, L. Li, X. Deng, W. Zhou, Z. Shao, A strongly coupled CoS_2/ reduced graphene oxide nanostructure as an anode material for efficient sodium-ion batteries, Journal of Alloys and Compounds 726 (2017) 394-402.
[111] X. Zhang, X. Jie Liu, G. Wang, H. Wang, Cobalt disulfide nanoparticles/graphene/carbon nanotubes aerogels with superior performance for lithium and sodium storage, J Colloid Interface Sci 505 (2017) 23-31.
[112] Y. Pan, X. Cheng, L. Gong, L. Shi, H. Zhang, Nanoflower-like N-doped C/CoS_2 as high-performance anode materials for Na-ion batteries, Nanoscale 10 (2018) 20813-20820.
[113] Y. Pan, X. Cheng, L. Gong, L. Shi, T. Zhou, Y. Deng, H. Zhang, Double-morphology CoS_2 anchored on N-doped multichannel carbon nanofibers as high-performance anode materials for Na-ion batteries, ACS Appl Mater Interfaces 10 (2018) 31441-31451.
[114] L. Shi, D. Li, P. Yao, J. Yu, C. Li, B. Yang, C. Zhu, J. Xu, SnS_2 nanosheets coating on nanohollow cubic CoS_2/C for ultralong life and high rate capability half/full sodium-ion batteries, Small 14 (2018) 1802716.

ACCEPTED MANUSCRIPT

[115] X. Wang, X. Li, Q. Li, H. Li, J. Xu, H. Wang, G. Zhao, L. Lu, X. Lin, H. Li, S. Li, Improved electrochemical performance based on nanostructured SnS_2@CoS_2-rGO composite anode for sodium-ion batteries, Nanomicro Lett 10 (2018) 46.
[116] Y. Lin, Z. Qiu, D. Li, S. Ullah, Y. Hai, H. Xin, W. Liao, B. Yang, H. Fan, J. Xu, C. Zhu, NiS_2@CoS_2 nanocrystals encapsulated in N-doped carbon nanocubes for high performance lithium/sodium ion batteries, Energy Storage Materials 11 (2018) 67-74.
[117] Y. Ma, Y. Ma, D. Bresser, Y. Ji, D. Geiger, U. Kaiser, C. Streb, A. Varzi, S. Passerini, Cobalt disulfide nanoparticles embedded in porous carbonaceous micro-polyhedrons interlinked by carbon nanotubes for superior lithium and sodium storage, ACS Nano 12 (2018) 7220-7231.
[118] R. Wu, D.P. Wang, X. Rui, B. Liu, K. Zhou, A.W. Law, Q. Yan, J. Wei, Z. Chen, In-situ formation of hollow hybrids composed of cobalt sulfides embedded within porous carbon polyhedra/carbon nanotubes for high-performance lithium-ion batteries, Adv Mater 27 (2015) 3038-3044.
[119] L. Zhou, K. Zhang, J. Sheng, Q. An, Z. Tao, Y.-M. Kang, J. Chen, L. Mai, Structural and chemical synergistic effect of CoS nanoparticles and porous carbon nanorods for high-performance sodium storage, Nano Energy 35 (2017) 281-289.
[120] Q. Zhou, L. Liu, G. Guo, Z. Yan, J. Tan, Z. Huang, X. Chen, X. Wang, Sandwich-like cobalt sulfide-graphene composite-an anode material with excellent electrochemical performance for sodium ion batteries, RSC Advances 5 (2015) 71644-71651.
[121] C. Wu, Y. Jiang, P. Kopold, P.A. van Aken, J. Maier, Y. Yu, Peapod-like carbon-encapsulated cobalt chalcogenide nanowires as cycle-stable and high-rate materials for sodium-ion anodes, Adv Mater 28 (2016) 7276-7283.
[122] X. Zhu, X. Jiang, X. Liu, L. Xiao, X. Ai, H. Yang, Y. Cao, Amorphous CoS nanoparticle/reduced graphene oxide composite as high-performance anode material for sodium-ion batteries, Ceramics International 43 (2017) 9630-9635.
[123] S. Peng, X. Han, L. Li, Z. Zhu, F. Cheng, M. Srinivansan, S. Adams, S. Ramakrishna, Unique cobalt sulfide/reduced graphene oxide composite as an anode for sodium-ion batteries with superior rate capability and long cycling stability, Small 12 (2016) 1359-1368.
[124] F. Han, C.Y. Jun Tan, Z. Gao, Template-free formation of carbon nanotube-supported cobalt sulfide@carbon hollow nanoparticles for stable and fast sodium ion storage, Journal of Power Sources 339 (2017) 41-50.
[125] Y. Zhang, C. Lv, X. Wang, S. Chen, D. Li, Z. Peng, D. Yang, Boosting sodium-ion storage by encapsulating NiS (CoS) hollow nanoparticles into carbonaceous fibers, ACS Appl Mater Interfaces 10 (2018) 40531-40539.
[126] J. Yu, X. Li, Y. Sun, X. Liu, CoS@sulfur doped onion-like carbon nanocapsules with excellent cycling stability and rate capability for sodium-ion batteries, Ceramics International 44 (2018) 17113-17117.
[127] Q. Guo, Y. Ma, T. Chen, Q. Xia, M. Yang, H. Xia, Y. Yu, Cobalt sulfide quantum dot embedded N/S-doped carbon nanosheets with superior reversibility and rate capability for sodium-ion batteries, ACS Nano 11 (2017) 12658-12667.
[128] X. Liu, H. Ma, Q. Liu, Y. Wang, Z. Lu, M. Li, J. Wang, D. Wang, Ethylenediamine-assisted synthesis of microsized cobalt sulfide as advanced anode materials for sodium ion batteries, Journal of Alloys and Compounds 735 (2018) 765-772.

ACCEPTED MANUSCRIPT

[129] Q. Li, L. Li, K.A. Owusu, W. Luo, Q. An, Q. Wei, Q. Zhang, L. Mai, Self-adaptive mesoporous CoS@alveolus-like carbon yolk-shell microsphere for alkali cations storage, Nano Energy 41 (2017) 109-116.
[130] S.-K. Park, J.K. Kim, Y.C. Kang, Excellent sodium-ion storage performances of $CoSe_2$ nanoparticles embedded within N-doped porous graphitic carbon nanocube/carbon nanotube composite, Chemical Engineering Journal 328 (2017) 546-555.
[131] X. Ma, L. Zou, W. Zhao, Tailoring hollow microflower-shaped $CoSe_2$ anodes in sodium ion batteries with high cycling stability, Chem Commun 54 (2018) 10507-10510.
[132] K. Zhang, M. Park, L. Zhou, G.-H. Lee, W. Li, Y.-M. Kang, J. Chen, Urchin-like $CoSe_2$ as a high-performance anode material for sodium-ion batteries, Advanced Functional Materials 26 (2016) 6728-6735.
[133] S.K. Park, Y.C. Kang, MOF-templated N-doped carbon-coated $CoSe_2$ nanorods supported on porous CNT microspheres with excellent sodium-ion storage and electrocatalytic properties, ACS Appl Mater Interfaces 10 (2018) 17203-17213.
[134] X. Ou, X. Liang, F. Zheng, P. Wu, Q. Pan, X. Xiong, C. Yang, M. Liu, In situ X-ray diffraction investigation of $CoSe_2$ anode for Na-ion storage: Effect of cut-off voltage on cycling stability, Electrochimica Acta 258 (2017) 1387-1396.
[135] J. Wang, H. Wang, D. Cao, X. Lu, X. Han, C. Niu, Epitaxial growth of urchin-like $CoSe_2$ nanorods from electrospun Co-embedded porous carbon nanofibers and their superior lithium storage properties, Particle & Particle Systems Characterization 34 (2017) 1700185.
[136] Y. Tang, Z. Zhao, X. Hao, Y. Wang, Y. Liu, Y. Hou, Q. Yang, X. Wang, J. Qiu, Engineering hollow polyhedrons structured from carbon-coated $CoSe_2$ nanospheres bridged by CNTs with boosted sodium storage performance, Journal of Materials Chemistry A 5 (2017) 13591-13600.
[137] J.S. Cho, J.M. Won, J.-K. Lee, Y.C. Kang, Design and synthesis of multiroom-structured metal compounds–carbon hybrid microspheres as anode materials for rechargeable batteries, Nano Energy 26 (2016) 466-478.
[138] J.K. Kim, J.H. Kim, Y.C. Kang, Electrochemical properties of multicomponent oxide and selenide microspheres containing Co and Mo components with several tens of vacant nanorooms synthesized by spray pyrolysis, Chemical Engineering Journal 333 (2018) 665-677.
[139] J. Gao, Y. Li, L. Shi, J. Li, G. Zhang, Rational design of hierarchical nanotubes through encapsulating $CoSe_2$ nanoparticles into $MoSe_2$/C composite shells with enhanced lithium and sodium storage performance, ACS Appl Mater Interfaces 10 (2018) 20635-20642.
[140] Y. Huang, Z. Wang, Y. Jiang, S. Li, Z. Li, H. Zhang, F. Wu, M. Xie, L. Li, R. Chen, Hierarchical porous $Co_{0.85}Se$@reduced graphene oxide ultrathin nanosheets with vacancy-enhanced kinetics as superior anodes for sodium-ion batteries, Nano Energy 53 (2018) 524-535.
[141] G. Zhang, K. Liu, S. Liu, H. Song, J. Zhou, Flexible $Co_{0.85}Se$ nanosheets/graphene composite film as binder-free anode with high Li- and Na-Ion storage performance, Journal of Alloys and Compounds 731 (2018) 714-722.
[142] Y. Zhang, A. Pan, L. Ding, Z. Zhou, Y. Wang, S. Niu, S. Liang, G. Cao, Nitrogen-doped yolk-shell-structured CoSe/C dodecahedra for high-performance sodium ion batteries, ACS Appl Mater Interfaces 9 (2017) 3624-3633.

ACCEPTED MANUSCRIPT

ACCEPTED MANUSCRIPT

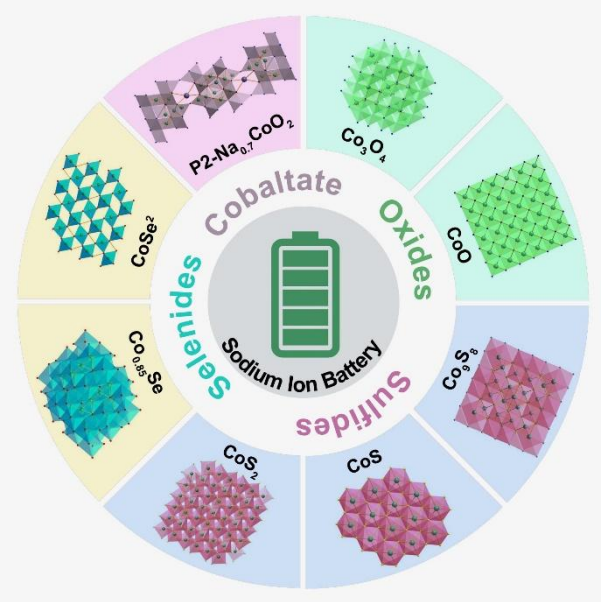
[143] J. Li, D. Yan, T. Lu, Y. Yao, L. Pan, An advanced CoSe embedded within porous carbon polyhedra hybrid for high performance lithium-ion and sodium-ion batteries, Chemical Engineering Journal 325 (2017) 14-24.
[144] X. Li, W. Zhang, Y. Feng, W. Li, P. Peng, J. Yao, M. Li, C. Jiang, Ultrafine CoSe nano-crystallites confined in leaf-like N-doped carbon for long-cyclic and fast sodium ion storage, Electrochimica Acta 294 (2019) 173-182.
[145] Z. Ali, T. Tang, X. Huang, Y. Wang, M. Asif, Y. Hou, Cobalt selenide decorated carbon spheres for excellent cycling performance of sodium ion batteries, Energy Storage Materials 13 (2018) 19-28.
[146] J. Wang, Z. Liu, Y. Zheng, L. Cui, W. Yang, J. Liu, Recent advances in cobalt phosphide based materials for energy-related applications, Journal of Materials Chemistry A 5 (2017) 22913-22932.
[147] W.-J. Li, Q.-R. Yang, S.-L. Chou, J.-Z. Wang, H.-K. Liu, Cobalt phosphide as a new anode material for sodium storage, Journal of Power Sources 294 (2015) 627-632.
[148] K. Zhang, M. Park, J. Zhang, G.-H. Lee, J. Shin, Y.-M. Kang, Cobalt phosphide nanoparticles embedded in nitrogen-doped carbon nanosheets: Promising anode material with high rate capability and long cycle life for sodium-ion batteries, Nano Research 10 (2017) 4337-4350.
[149] Q. Li, S. Dong, Y. Zhang, S. Feng, Q. Wang, J. Yuan, Ultrafine CoP Nanoparticles anchored on reduced graphene oxide nanosheets as anodes for sodium ion batteries with enhanced electrochemical performance, European Journal of Inorganic Chemistry 2018 (2018) 3433-3438.
[150] Z. Li, L. Zhang, X. Ge, C. Li, S. Dong, C. Wang, L. Yin, Core-shell structured CoP/FeP porous microcubes interconnected by reduced graphene oxide as high performance anodes for sodium ion batteries, Nano Energy 32 (2017) 494-502.
[151] J. Zhang, K. Zhang, J. Yang, G.-H. Lee, J. Shin, V. Wing-hei Lau, Y.-M. Kang, Bifunctional conducting polymer coated CoP core-shell nanowires on carbon paper as a free-standing anode for sodium ion batteries, Advanced Energy Materials 8 (2018) 1800283.
[152] X. Ge, Z. Li, L. Yin, Metal-organic frameworks derived porous core/shell CoP@C polyhedrons anchored on 3D reduced graphene oxide networks as anode for sodium-ion battery, Nano Energy 32 (2017) 117-124.
[153] Y. Nagata, K. Nagao, M. Deguchi, A. Sakuda, A. Hayashi, H. Tsukasaki, S. Mori, M. Tatsumisago, Amorphization of sodium cobalt oxide active materials for high-capacity all-solid-state sodium batteries, Chemistry of Materials 30 (2018) 6998-7004.
[154] Z. Li, J. Yang, J.G. Hou, Q. Zhu, First-principles lattice dynamics of $NaCoO_2$, Physical Review B 70 (2004).
[155] M. Medarde, M. Mena, J.L. Gavilano, E. Pomjakushina, J. Sugiyama, K. Kamazawa, V.Y. Pomjakushin, D. Sheptyakov, B. Batlogg, H.R. Ott, M. Mansson, F. Juranyi, 1D to 2D Na^+ ion diffusion inherently linked to structural transitions in $Na_{0.7}CoO_2$, Phys Rev Lett 110 (2013) 266401.
[156] J.J. Braconnier, C. Delmas, C. Fouassier, P. Hagenmuller, Comportement electrochimique des phases Na_xCoO_2, Materials Research Bulletin 15 (1980) 1797-1804.
[157] R. Berthelot, D. Carlier, C. Delmas, Electrochemical investigation of the P2-Na_xCoO_2 phase diagram, Nat Mater 10 (2011) 74-80.
[158] C. Delmas, J.J. Braconnier, C. Fouassier, P. Hagenmuller, Electrochemical intercalation of sodium in Na_xCoO_2 bronzes, Solid State Ionics 3 (1981) 165-169.

ACCEPTED MANUSCRIPT

[159] L. Shacklette, T. Jow, L. Townsend, Rechargeable electrodes from sodium cobalt bronzes, Journal of The Electrochemical Society 135 (1988) 2669-2674.
[160] S. Kalluri, M. Yoon, M. Jo, S. Park, S. Myeong, J. Kim, S.X. Dou, Z. Guo, J. Cho, Surface engineering strategies of layered $LiCoO_2$ cathode material to realize high-energy and high-voltage Li-ion cells, Advanced Energy Materials 7 (2017) 1601507.
[161] N. Yabuuchi, K. Kubota, M. Dahbi, S. Komaba, Research development on sodium-ion batteries, Chemical Reviews 114 (2014) 11636-11682.
[162] N. Sabi, A. Sarapulova, S. Indris, H. Ehrenberg, J. Alami, I. Saadoune, Effect of titanium substitution in a P2-$Na_{2/3}Co_{0.95}Ti_{0.05}O_2$ cathode material on the structural and electrochemical properties, ACS Appl Mater Interfaces 9 (2017) 37778-37785.
[163] Y.J. Fang, X.Y. Yu, X.W. Lou, A practical high-energy cathode for sodium-ion batteries based on uniform P2-$Na_{0.7}CoO_2$ microspheres, Angewandte Chemie-International Edition 56 (2017) 5801-5805.
[164] L. Gao, S. Chen, L. Zhang, X. Yang, Self-supported $Na_{0.7}CoO_2$ nanosheet arrays as cathodes for high performance sodium ion batteries, Journal of Power Sources 396 (2018) 379-385.
[165] S. Doubaji, L. Ma, H.D. Asfaw, I. Izanzar, R. Xu, J. Alami, J. Lu, T. Wu, K. Amine, K. Edstrom, I. Saadoune, On the P2-$Na_xCo_{1-y}(Mn_{2/3}Ni_{1/3})_yO_2$ cathode materials for sodium-ion batteries: synthesis, electrochemical performance, and redox processes occurring during the electrochemical cycling, ACS Appl Mater Interfaces 10 (2018) 488-501.
[166] S.C. Han, H. Lim, J. Jeong, D. Ahn, W.B. Park, K.-S. Sohn, M. Pyo, Ca-doped Na_xCoO_2 for improved cyclability in sodium ion batteries, Journal of Power Sources 277 (2015) 9-16.
[167] M. Matsui, F. Mizukoshi, N. Imanishi, Improved cycling performance of P2-type layered sodium cobalt oxide by calcium substitution, Journal of Power Sources 280 (2015) 205-209.
[168] M. Bianchini, J. Wang, R. Clément, G. Ceder, A first-principles and experimental investigation of nickel solubility into the P2 Na_xCoO_2 sodium-ion cathode, Advanced Energy Materials 8 (2018) 1801446.
[169] S.M. Kang, J.H. Park, A. Jin, Y.H. Jung, J. Mun, Y.E. Sung, Na^+/vacancy disordered P2-$Na_{0.67}Co_{1-x}Ti_xO_2$: high-energy and high-power cathode materials for sodium ion batteries, ACS Appl Mater Interfaces 10 (2018) 3562-3570.
[170] V.K. Singh, S.K. Singh, H. Gupta, Shalu, L. Balo, A.K. Tripathi, Y.L. Verma, R.K. Singh, Electrochemical investigations of $Na_{0.7}CoO_2$ cathode with PEO-NaTFSI-BMIMTFSI electrolyte as promising material for Na-rechargeable battery, Journal of Solid State Electrochemistry 22 (2018) 1909-1919.

ACCEPTED MANUSCRIPT

ACCEPTED MANUSCRIPT



ACCEPTED MANUSCRIPT

ACCEPTED MANUSCRIPT

Highlights

A comprehensive review of the recent progress with cobalt-based electrodes for sodium-ion batteries is presented.

The electrochemical mechanisms are pointed out.

The relationship between crystalline structure and electrochemical performance are discussed.

The strategies to enhance the overall electrochemical performance of cobalt-based cathode and anode materials are discussed.

ACCEPTED MANUSCRIPT